Fermi National Accelerator Laboratory

FERMILAB-Pub-89/200-E
[E-665]

A Spectrometer for Muon Scattering at the Tevatron*

The E-665 Collaboration

M.R. Adams[7], S. Aid[8], P.L. Anthony[9], M.D. Baker[9], J.F. Bartlett[4], A.A. Bhatti[11], H.M. Braun[12], T. Burnett[11], W. Busza[9], J.M. Conrad[6], G.B. Coutrakon[4,a], R. Davisson[11], S.K. Dhawan[13], W. Dougherty[11], T. Dreyer[5], U. Ecker[12], V. Eckardt[10], M. Erdmann[5], A. Eskreys[3], K. Eskreys[3], H.J. Gebauer[10], D.F. Gessaman[1], R. Gilman[1], M.C. Green[1,b], J. Haas[5], C. Halliwell[7], J. Hanlon[4], V.W. Hughes[13], H.E. Jackson[1], D.M. Jansen[11], G. Jansco[10], S. Kaufman[1], R.D. Kennedy[2], T. Kirk[4], H. Kobrak[2], S. Krzywdzinski[11,c], S. Kunori[8], J. Lord[11], H.J. Lubatti[11], T. Lyons[9], S. Magill[7], P. Malecki[3], A. Manz[10], D. McLeod[7], H. Melanson[4], D.G. Michael[6], W. Mohr[5], H.E. Montgomery[4], J.G. Morfín[4], R.B. Nickerson[6], S. O'Day[8], A.M. Osborne[2,4,6,d], L. Osborne[9], B. Pawlik[3], F.M. Pipkin[6], E.J. Ramberg[8], A. Röser[12], J. Ryan[9], A. Salvarani[2], M. Schmitt[6], K.P. Schüler[13], E. Sexton[2,7,e], H.J. Seyerlein[10], A. Skuja[8], S. Söldner-Rembold[10], P.H. Steinberg[8,f], H.E. Stier[5], P. Stopa[10,g], P. Strube[10], Robert A. Swanson[2], R.L. Talaga[8,h], S. Tentindo-Repond[1,i], H.-J. Trost[10,h], H. Venkataramania[13], M. Vidal[10], M. Wilhelm[5], J. Wilkes[11], Richard Wilson[6], S. Wolbers[4], T. Zhao[11]

1 *Argonne National Laboratory, 9700 S. Cass Avenue, Argonne, Illinois 60439 U.S.A.*
2 *University of California, San Diego, La Jolla, California 92093 U.S.A.*
3 *Institute of Nuclear Physics and Institute of Nuclear Physics & Technology, Ul. Kawiory 26a PL-30-055 Cracow Poland*
4 *Fermi National Accelerator Laboratory, P.O. Box 500, Batavia, Illinois 60510 U.S.A.*
5 *University of Freiburg i.Br., D-7800 Freiburg 33, Germany*
6 *Harvard University, Cambridge, Massachusetts 02138 U.S.A.*
7 *University of Illinois at Chicago, Chicago, Illinois 60680 U.S.A.*
8 *University of Maryland, College Park, Maryland 20742 U.S.A.*
9 *Massachusetts Institute of Technology, Cambridge, Massachusetts 02139*
10 *Max Planck Institute for Physics and Astrophysics, D-8000 Munich 40, Germany*
11 *University of Washington, Seattle, Washington 98195 U.S.A.*
12 *University of Wuppertal, D-5600 Wuppertal 1, Germany*
13 *Yale University, New Haven, Connecticut 06511* U.S.A.

May 1989

*Submitted to Nucl. Instrum. Methods

A SPECTROMETER FOR MUON SCATTERING AT THE TEVATRON

E665 Collaboration
May 1989

M.R. Adams[7], S. Aid[8], P.L. Anthony[9], M.D. Baker[9], J.F. Bartlett[4], A.A. Bhatti[11], H.M. Braun[12], T. Burnett[11], W. Busza[9], J.M. Conrad[6], G.B. Coutrakon[4,a], R. Davisson[11], S.K. Dhawan[13], W. Dougherty[11], T. Dreyer[5], U. Ecker[12], V. Eckardt[10], M. Erdmann[5], A. Eskreys[3], K. Eskreys[3], H.J. Gebauer[10], D.F. Geesaman[1], R. Gilman[1], M.C. Green[1,b], J. Haas[5], C. Halliwell[7], J. Hanlon[4], V.W. Hughes[13], H.E. Jackson[1], D.M. Jansen[11], G. Jancso[10], S. Kaufman[1], R.D. Kennedy[2], T. Kirk[4], H. Kobrak[2], S. Krzywdzinski[11,c], S. Kunori[8], J. Lord[11], H.J. Lubatti[11], T. Lyons[9], S. Magill[7], P. Malecki[3], A. Manz[10], D. McLeod[7], H. Melanson[4], D.G. Michael[6], W. Mohr[5], H.E. Montgomery[4], J.G. Morfin[4], R.B. Nickerson[6], S. O'Day[8], A.M. Osborne[2,4,6,d], L. Osborne[9], B. Pawlik[3], F.M. Pipkin[6], E.J. Ramberg[8], A. Röser[12], J. Ryan[9], A. Salvarani[2], M. Schmitt[6], K. P. Schüler[13], E. Sexton[2,7,e], H.J. Seyerlein[10], A. Skuja[8], S. Söldner-Rembold[10], P.H. Steinberg[8,f], H.E. Stier[5], P. Stopa[10,g], P. Strube[10], Robert A. Swanson[2], R.L. Talaga[8,h], S. Tentindo-Repond[1,i], H.-J. Trost[10,h], H. Venkataramania[13], M. Vidal[10], M. Wilhelm[5], J. Wilkes[11], Richard Wilson[6], S. Wolbers[4], T. Zhao[11]

1 Argonne National Laboratory
2 University of California, San Diego
3 Institute of Nuclear Physics, Cracow, Poland
& Institute of Nuclear Physics & Technology, Cracow, Poland
4 Fermi National Accelerator Laboratory
5 University of Freiburg i.Br.
6 Harvard University
7 University of Illinois at Chicago
8 University of Maryland, College Park
9 Massachusetts Institute of Technology
10 Max Planck Institute for Physics & Astrophysics, Munich
11 University of Washington, Seattle
12 University of Wuppertal
13 Yale University

ABSTRACT

In this paper the spectrometer constructed by the E665 collaboration is described. The spectrometer was built during the period 1982-87 and the first data were taken during the 1987-88 Fixed Target run of the Fermi National Accelerator Laboratory (FNAL) Tevatron. This is the first of a series of runs in which a comprehensive program of high energy muon scattering experiments will be performed.

a Current address: Loma Linda Univ. Medical Center, Loma Linda, California.
b Current address: LeCroy Research Systems, Spring Valley, NY 10977.
c Current address: FNAL, PO Box 500, Batavia, IL 60510.
d Permanent address: CERN, 23 Geneve 1211, Switzerland.
e Current address: FNAL, PO Box 500, Batavia, IL 60510.
f Deceased.
g Permanent address: Institute of Nuclear Physics, Cracow, Poland.
h Current address: H.E.P. Div., ANL, Argonne, IL 60439-4843.
i Current address: Northern Illinois University, Dekalb, IL 60115.

INTRODUCTION

The use of charged lepton beams as tools to probe the deepest structure of matter has proved to be a fruitful line of research. A series of experiments [1,2,3,4] has been performed at the high energy proton accelerators at FNAL and CERN using muon beams. This paper describes the apparatus used in the most recent and highest energy experiments in this series. The detector is installed in the NM beamline at the Tevatron. The following sections describe the general layout of the beamline and spectrometer and also details of individual components. These include the beam and the beam tagging spectrometer, the targets, the tracking chambers, the particle identification detectors, the electromagnetic calorimeter, the muon detection, the triggering systems, and the readout and online monitoring systems. The purpose of the paper is to give an overview of the apparatus and aspects of its performance. It is expected that readers will refer to specific publications for the innovative and detailed aspects of the individual elements.

In the main body of the paper the apparatus is described as it was used during the July 1987 to February 1988 Fixed Target running period. Modifications that are being made in preparation for the next Fixed Target run are also briefly outlined.

The internal E665 notation for each detector will be used for brevity; this notation will be defined with the introduction of each detector. The coordinate system used is right handed: X is along the nominal beam direction, Y is horizontal, Z is vertical with positive up. When a Z or Y plane of a detector is referenced, the plane measures the coordinate indicated; thus Z planes have horizontal wires or counter fingers.

GENERAL DESCRIPTION

The layout of the NM beam is shown in Figure 1. It has a total length of approximately 1.5 km. Those muons used as beam by the experiment are defined by the beam spectrometer, which is based on the last bend (θ_{bend} = 3 mr) in the beamline. 80% of the muons in the beamline are inside an area which is defined as useful beam. For muon scatters at large angle ($\theta_{scat} > 3$ mr) the exact muon trajectory within this area is determined only during analysis. However, for small angles of scatter (θ_{scat} down to 0.5 mr), it is necessary to measure individual muon trajectories as part of the beam definition during data taking.

The experimental apparatus, which is shown in Figure 2 and summarized in table 1, is built around two large superconducting dipole magnets. The first, the Cern Vertex Magnet, CVM, was used in the NA9 muon scattering experiment [5] at CERN. The second, the Chicago Cyclotron Magnet, CCM, has a long history of utilization in particle physics [1] and was used in previous muon experiments at FNAL. The field directions in the two magnets are of opposite orientation and their magnitudes are arranged to form a focussing condition (Trigger section). These two magnets combined, in conjunction with associated particle detectors, provide high resolution momentum measurement of particles from 100 MeV/c up to the incident muon momentum. Low momentum particles (<500 MeV/c) do not exit the magnetic field of the CVM. The angular acceptance of the spectrometer in the laboratory starts at zero (the incident muon direction) and, for some events, extends to more than 150°; in the center of mass of the interaction this is almost 4π steradians.

The muon beam impinges on a target located within the field of the CVM. In the phase of the experiment designed to study final state hadrons, targets are chosen such that the hadrons exit from the target with only a small probability of reinteraction. A streamer chamber, SC, surrounds the target. Immediately downstream of the CVM is a six plane multi-wire proportional chamber, PCV. At large angles the particles encounter a time of flight detector, TOF; four planes of proportional tube detectors, PTA; and a gas threshold Cherenkov counter C0. At smaller angles there is a second gas threshold Cherenkov detector, C1. These detectors provide particle identification in the momentum range 300 MeV/c to 30 GeV/c. With the exception of the PTA tubes all of the detectors deployed around the CVM were used in the NA9 experiment at CERN; in this paper those aspects of the spectrometer which are particular to E665 are emphasized.

Downstream of this vertex spectrometer the forward going particles traverse a series of multi-wire proportional chambers. The PC chambers (twelve planes) are in the field free region between the two magnets. The PCF detectors (fifteen planes) are in the gap of the CCM magnet. Immediately after the CCM are four drift chamber packages, DC1-4 (two planes each). Eight meters downstream are four more sets of drift chambers, DC5-8 (two planes each). The drift chambers are deadened in the beam region. This hole is covered by two sets of proportional wire chambers, PSB and PSA, (four and eight planes respectively); PSB is situated just upstream of the second set of drift chamber packages and PSA just downstream. The combination of these wire chamber detectors downstream

of the vertex spectrometer provides pattern recognition and momentum measurement for charged particles with momentum greater than a few GeV/c. The angular resolution is 100 μr and the momentum resolution is $\delta p/p = p \times 5 \times 10^{-5}$, ($p$ in GeV/c).

Between the two banks of drift chambers is a gas ring-imaging Cherenkov counter, RICH. This extends the charged particle identification capability of the spectrometer up to the 100 GeV/c region; the exact momentum limit depends on the radiator gas in use.

An electromagnetic calorimeter, CAL, is downstream of DC8 and PSA and provides electromagnetic particle detection.

Immediately downstream of CAL, the hadrons are absorbed in a 3.0 m thick iron wall. After the iron, the muons encounter four identical sets of detectors with 90 cm thick concrete walls separating them. Each set contains, in order: two orthogonal planes of proportional tubes, PTMY1-4 and PTMZ1-4, which are deadened in the beam region; two orthogonal hodoscopes of scintillators, SMSY1-4 and SMSZ1-4, at small angles; and a plane of scintillation counters, SPM1-4, at large angles. These four detector packages permit the identification of muons by track matching through the absorbers. Scattered muon triggering of data acquisition is also based on the detectors behind the iron hadron absorber.

THE BEAM

The NM beam has been discussed extensively elsewhere [6] and is shown schematically in Figure 1. The proton beam impinges on a target of 48.5 cm of beryllium. Transmitted protons are separated from the secondary hadrons and are dumped in an absorber. The pions (and kaons) are momentum selected and transported in a Focussing-Defocussing channel, FODO, for 1.1 km. For 800 GeV/c protons incident on the target, approximately 5% of the secondaries decay to produce muons which remain in the FODO. The hadrons which do not decay are absorbed in a piece of beryllium, 11 m long, leaving only the muons. These enter a second FODO channel in which they are transported 420 m to the experiment.

In addition to useful muons, a widely dispersed spray of muons outside the nominal beam is produced. These muons are termed the halo and are always associated with a muon beam. A large fraction of these are steered away from the experiment using a magnetic deflection scheme. Within the second (muon) FODO, four sections of a special

casing, MUPIPE, (33 m total) is installed around the beam pipe. MUPIPE is a thick-walled steel pipe magnetized with a strong (2.0 T) toroidal field. Muons which are not contained within the bore of the pipe are deflected radially and on average encounter about 7 Tm of toroidal magnetic field before leaving the pipe. The initial deviation generated by the MUPIPE is then augmented by 15 m of larger diameter toroids. During the 1987–88 running period, the experiment detected approximately as many muons in the halo as in the beam when the MUPIPE and toroids were demagnetized. With them magnetized, (the normal situation), the halo was reduced to a total of 20–30% of the useful beam. About half of this halo was contained within a radius of 20 cm from the nominal beam axis and the rest was spread over the 7 m×3 m sensitive area of the muon detector.

The performance of the beam, including the muon flux at different momenta, is summarized in Table 2. It should be noted that the definition of useful muon flux is measurement dependent, so that care must be taken in interpreting the numbers. In particular the 100 GeV/c beam was not optimized due to radiation safety restrictions.

The beam has a transverse size of approximately 3 cm (Figure 3). For some energies the incident muon flux can reach $> 2 \times 10^8$ muons per Tevatron cycle. Since the length of the proton extraction is 20 s (the spill length), instantaneous rates over 10^6 s^{-1} per millimeter wide section of the beam are possible. During the 1987–88 period the maximum beam intensity was 2×10^7/spill, and the machine cycle time was 57 s.

Another important feature of the Tevatron muon beam is that it preserves the RF time structure generated by the radio frequency system of the accelerator. The RF is 53 MHz (RF Phase Locking section) giving RF buckets spaced at 19 ns intervals. As a result the muons are spaced 19 ns apart in time with a jitter which is less than 1 ns. This structure proves to be of considerable utility in the logic used to trigger the experiment. One limitation, however, is that at the highest beam intensities about 20% of the occupied RF buckets contain more than one muon. The beam spectrometer is designed to accommodate this situation.

The NM beamline can also be used to transport hadrons and electrons for calibration purposes (Calibration and Alignment section). Beamline modifications are made to produce electrons for calibration [7]: a secondary target is installed 60 m upstream of the beryllium absorber; a dipole magnet just downstream of the secondary target sweeps

charged particles out of the beam; the beryllium absorber is replaced with 0.1 radiation lengths of lead. The resulting electrons and positrons are transported along the muon FODO to the experiment. The electrons are tagged in the beam spectrometer in the same way as the muons, but with a lower current in the tagging magnet. A final dipole magnet, which can be rotated remotely, is used to alter the direction of the beam as it enters the experimental hall.

§*Beam Spectrometer*

The function of the beam spectrometer is twofold. It must provide a fast signal for the trigger logic when a useful beam muon has entered the experiment and it must provide the information from which the incident muon momentum and trajectory are reconstructed during analysis. To serve these purposes, the beam spectrometer is composed of four measurement stations, BMS1-4, situated with lever arms of approximately 27 m on either side of the final 3 mr dipole bend in the muon beam. The layout is shown in Figure 1.

Each station contains six multiwire proportional chamber planes, PBT, [8] which have 1 mm wire spacing, with orientations U(+30°) Z, Y, V(−30°), Z′ (offset by 0.5 mm), and Y′ (see Figure 4). The six planes are organized into two separate gas volumes with independent high voltage supplies; the arrangement is such that if a single plane fails, the second set of chambers can still provide a Y−Z point. The Y and Z planes have sensitive areas of ∼12.8 cm×12.8 cm, while the inclined planes are sensitive over ∼ 6.4 cm×14 cm. The chambers are operated with the cathode planes at −3.1 kV. The anode wires are 10 μm gold plated tungsten and are at ground potential. The gas mixture is 50% argon, 50% ethane bubbled through ethanol at 0°C. The signals from the chambers are amplified and discriminated at the chambers (NAN† N277) and the discriminated signals are transmitted to delay/latch modules (LRS‡ 2731A, PCOS III MWPC Readout System).

All stations are equipped with scintillation counter hodoscopes, SBT: Y views in all stations (the bend plane) and Z views in stations one, three and four. All Y views and the Z views in stations three and four have thirteen counters, the size of which are graded in order to have approximately equal rates in each finger (Figure 4). These hodoscopes are used in the experiment trigger logic; in addition, they may be used to mask the hits

† NAN: Nanometric Systems Inc.

‡ LRS: LeCroy Research Systems Corp.

in the PBT chambers and eliminate tracks and hits associated with other RF buckets. The Z hodoscope in station one also has thirteen counters, but in this case they are of equal size in order to enhance the beam fraction which may be used by the small angle trigger (Trigger section). The signals from the photomultiplier tubes (HAM† R1398) are transmitted to a position adjacent to the most downstream station in the system. Here the signals are passively split. One half is discriminated (LRS4416) and the resulting logic signals are transmitted to both the trigger circuitry and to latches (LRS4448). The other half of the analog signal is digitized (LRS2249), which provides a monitor of the latch system and useful diagnostic information for the counters.

The ensemble of detectors is intended to operate in a beam flux of up to 2×10^8 beam particles per spill and is capable of reconstructing multiple beam particles in the same RF bucket. The resolution in angle is about 10 μr and in momentum about 0.5%, independent of the beam momentum tune since the bend is always 3 mr. During the 1987–88 run the reconstruction efficiency for beam muons was in excess of 99% for events with a single muon in the beam spectrometer. This efficiency does not affect the experiment normalization.

HALO VETO SYSTEM

The halo muons associated with the beam (Beam section) are potential sources of background in the various physics triggers used by the experiment. In order to reduce problems associated with halo muons, an array of scintillation counters is arranged around the beam to detect muons outside the useful phase space. Signals from the scintillators are used to veto spurious triggers associated with halo muons. The system has two components: a large array of counters with a hole slightly larger than any foreseen useable beam, and a set of smaller arrays which have an adjustable aperture, which are used to define the size of the useful beam under some circumstances.

The large scintillation counter wall, SVW, is constructed of twenty eight counters, each 1.5 m×0.55 m, situated approximately 5.0 m upstream of the CVM center. The total area covered by these counters (7 m×3 m) adequately shadows the scattered muon detector. The central four counters are cut so that the beam enters the apparatus through a 25 cm×25 cm hole in the wall. The signals from the counters are split in the same manner as the SBT hodoscopes, producing both logic and analog signals. The counters

† HAM: Hamamatsu Photonics K.K.

have RCA† 8575 phototubes. Discrimination, latching, and signal digitization is done with LRS 4416, 4448, and 2249 modules respectively. A source of accidental signals in the SVW wall is low energy particles accompanying the muon beam. To help suppress this effect, the SVW counters are mounted on the downstream side of a 5 cm thick steel wall. The steel has a hole in it which matches the size of the hole in the counter array.

Three pairs of scintillation counters, SVJ1-3, close to the beam, complete the halo veto system. These are located at stations two, three and four of the beam tagging spectrometer. Each pair covers 50 cm×50 cm around the beam with an adjustable aperture (Figure 4) for the passage of the beam. The counters use RCA6655 tubes and use the same discrimination and readout scheme as the SVW counters. Due to their close proximity to the beam, the SVJ counters have comparatively high rates. Up to 5% of the muon flux traverses a single SVJ counter.

TARGETS

The initial program for the experiment involves the study of hadrons produced by muons. Hydrogen, deuterium, and a series of higher atomic number targets are being used. In addition to single target studies, the range of targets allows investigation of A-dependence effects; these occur both in structure functions and in final state hadron production. To study the final state hadrons a relatively thin target is required; a thick target would result in a large fraction of the hadrons re-interacting in the target. Typical target thicknesses are in the range 10 g/cm^2 - 20 g/cm^2. Targets with high atomic number produce more electromagnetic interactions and cause proportionately more spurious triggers than low atomic number targets.

At different times during the 1987–88 data taking period two target vessels and three targets were used. A cryogenic liquid target 1.1 m long and 9 cm in diameter was positioned inside the streamer chamber. It was used with both hydrogen and deuterium during the 1987–88 run. The target density was calculated from the measured vapor pressure in the reservoir vessel. It was also determined that boiling did not cause a significant change in the target density. The end-walls of the target vessel were 1 mm of Kapton, which is 2% of the thickness in grams of the hydrogen filling. Thus the spurious event rate from

† RCA: RCA Tube Operations.

the target vessel was small and was measured by taking data with the vessel filled with atmospheric pressure helium.

A pressurized-gas target, 1.12 m long and 7.2 cm in diameter was also used inside the streamer chamber and was filled with xenon at a pressure of 14atm. At this pressure about 9.5 g/cm^2 of xenon is in the target, which is comparable to the thickness of the hydrogen cryogenic target and half that of the deuterium target. The vessel was constructed of 200 μm mylar reinforced with Kevlar† and epoxy, yielding a wall 1 mm thick. The thickness of the target vessel in the beam was 0.3 g/cm^2 or 5% of the total target thickness.

Table 3 lists the salient features of the targets that were used during the 1987–88 data run.

TRACKING DETECTORS

§ *The SC Streamer Chamber*

The streamer chamber, SC, has been used in previous experiments [5]. It has an active volume of 2.0 m×1.2 m×0.7 m. A three gap system permits insertion of various targets in the beam and avoids an electrode in the median plane, where the track density is high. The high voltage pulses applied to the electrodes are ±350 kV, 10 ns long, and are generated by a Marx and Blumlein system. The generation time for the high voltage pulse is 400 ns, and the chamber memory time is adjusted to be ~1 μs by changing the gas mixture. Pulse generation is started 600 ns after the passage of the incident muon so that electromagnetic radiation from the process does not generate significant noise in other detectors. The ~1 μs memory means that each picture contains several muon beam tracks not associated with the trigger. These extra tracks are easily identified and do not cause difficulties during analysis.

The Marx generator requires several hundred milliseconds to recharge so that normal operation of the system is at a trigger rate of about 1.5 s^{-1}.

The chamber is viewed from above by three cameras with small stereo angles (12° and 15°). Streamer brightness is enhanced by the use of two stage image intensifiers. The demagnification between chamber and film is 1/66 at the median plane. The two track resolution is ~3 mm in space and is dominated by the apparent streamer width.

† DuPont Corporation.

Single track position measurements are accurate to ~850 μm in space, giving a momentum resolution of $\delta p/p = p \times 10^{-2}$, ($p$ in GeV/c). Figure 5 shows a typical streamer chamber picture for a 500 GeV/c muon interaction in hydrogen.

§*The PCV Proportional Chamber*

The PCV multi-wire proportional chamber [9] is a copy of a chamber used in the NA9 experiment [5]; it is mounted in the downstream aperture of the CVM magnet. It has a sensitive area of 2.8 m×1.0 m, and the package contains six planes. The plane orientations are: Y, U(+45°), U'(+18.5°), V(-18.5°), V'(-45°), and Y. Wire separation is 2 mm, and the cathodes are constructed of foam (ROHM† Rohacell) planes covered with mylar. The mylar is coated with a thin film of graphite. This construction minimizes the amount of material needed in the support frame, which is in the acceptance of wide angle tracks seen by the Time of Flight system. The gas mixture used is argon 71.8%, isobutane 28%, $CBrF_3$‡ 0.14% and trace isopropyl alcohol. In total the six planes have a thickness of 0.49 g/cm^2 in their active region. Output signals travel along 6.6 m of cable to preamplifiers; a further 65 m of cable takes the signals to electronics where they are amplified, discriminated and delayed using a monostable circuit. The data are then latched and encoded. The single plane efficiency for detecting halo muons away from the beam region during low intensity running is typically 90% for the subset of the 1987–88 data examined.

§*The PTA Proportional Tubes*

There are two banks of proportional tube counters (four planes each) located behind the TOF arrays. The PTA proportional tube planes are of identical construction to the PTM tube planes described below (Muon identification section); only the position, size and orientation is different. Each wall of PTAs has four planes of tubes (eight layers of wires). They are oriented with Z, Y, U(+45°) and V(-45°) views. The active area is 2 m×2 m. Readout and digitization is as for the PTM tubes.

---

† ROHM: Rohm GmbH, Chemische Fabrik

‡ The chemical formula is quoted for gases that are often referenced by the trade name "Freon"

§*The PC Proportional Chambers*

The PC proportional chambers were used in an earlier experiment, NA24 [10]. The system consists of three packages of four planes. Each package has an independent gas volume and contains planes with Y, Z, U(+28°), and V(−28°) orientations. The anode wire spacing is 3 mm, and the sensitive area of the chambers is 2 m×2 m. The cathodes are constructed from plastic foils stretched on "Stesalit" frames and sprayed with a graphite coating on each face. The gas mixture employed is the same as for PCV. Together, the twelve planes have a total thickness of 0.33 g/cm^2 in the active region. The preamplifiers are mounted directly on the chambers and drive twisted pair cables which go to the RMH [11] readout system. RMH crates contain the amplifiers, discriminators and latches. An encoder for the complete system is housed in CAMAC. Each group of thirty two wires forms a fast OR which is used for triggering, as described in the section on triggers. The average efficiency for detecting muons in the halo for the subset of the 1987−88 data examined is ∼85% per plane.

§*The PCF Proportional Chambers*

The PCF system [12] consists of five triplets of multiwire proportional chambers distributed in the upstream part of the CCM magnet (see Figure 2). Each triplet contains a U(+15°), V(−15°) and Z plane. Each plane within a triplet is self-contained with gas volume and cathode planes. The wire diameter is 20 μm, interwire spacing is 2 mm, the anode to cathode gap is 6.4 mm, and the spacing along X between successive planes in a triplet is 6.7 cm. The cathode planes are aluminized Kapton sheets glued to 1.27 cm thick styrofoam which is backed with aluminized mylar. The total sensitive area of each chamber is 2 m×1 m, and each triplet is 0.5 g/cm^2 thick in the active region. There are two support wires in each Z plane, one either side of the beam region. The U and V planes have a single support wire, which is located near the center of the chambers. Support wires are at different locations in each plane. The gas mixture used in the chambers is 80% argon, 19.7% carbon-dioxide, and 0.3%, $CBrF_3$ at atmospheric pressure. The high voltage is typically 3.8 kV.

Wire signals are amplified and discriminated (NAN N-303) on the chambers. The discriminated signals are delayed by monostables (700 ns), stored and read out from shift

registers. Readout and data reduction is performed in parallel from each triplet and serially within a triplet using five NAN WCS-300 scanners.

The average single-plane efficiency for detecting muons in the halo away from the beam region and support wires is >95% for the subset of the 1987−88 data examined to date.

§*The DC1-8 Drift Chambers*

The chamber packages DC1-8 [13] are drift chambers with drift cells 50.8 mm wide in the drift direction and 9.6 mm along the beam direction. The sense wires are 20 μm gold plated tungsten and are operated at a high voltage of 1.8 kV. Wire placement was controlled to a precision of 100 μm during construction. The drift field is 492 V/cm and the gas mixture is 50% argon, 50% ethane bubbled through ethanol at 0°C. This results in a drift speed of $\sim$4 cm/μs. Individual wire chamber packages contain two planes both measuring the same view but offset by half a drift cell. DC1-8 are organized into two groups of four, each of which has four Z planes, two U planes (+5.758°), and two V planes (-5.785°). Z wires are separated at a G10 septum located midway across the chamber, and each side is read out separately; this improves the multi-hit capability of the system. DC1-4 have a sensitive area of 2 m×4 m. DC5-8 have a sensitive area of 2 m×6 m. The beam region is deadened in each plane, with a dead region of average size 10 cm in Y and 5 cm in Z. Each eight plane package has a total thickness of 0.045 g/cm^2 in the sensitive area.

The signals on the wires are amplified and discriminated (NAN N-311) on the chambers with a double pulse resolution of 100 ns. Discriminated signals are transmitted on 28 m of twisted pair cables to a repeater, after which there is another 32 m of cable to the time digitizer. The digitizer is a common start, multi-hit system with 2 ns resolution [14]. After calibration using halo muon events, the spatial resolution is $\sim$400 μm. Individual wire corrections have not yet been applied; implementing these will result in considerable improvement in the spatial resolution. The efficiency for detecting halo muons away from the beam region during low intensity running is 95%±4% for the subset of the 1987−88 data examined.

§*The PSA,PSB Small Angle Chambers*

The PSA chambers consist of two identical four plane packages of proportional chambers based on the same design [8] as those used for the beam spectrometer. They are

located between DC8 and CAL. The first 4 plane package is mounted with orientation Z, Y, Z′ and Y′ (primed planes are offset by 0.5 mm). The second package is mounted at 45° with respect to the first, resulting in U (+45°), V(−45°), U′ and V′ orientations. The planes have 1 mm wire spacing and an active area of ~12.8 cm×12.8 cm, which adequately covers the dead region of the drift chambers. The average thickness of each four plane package is 9.3 g/cm^2, including the support frames and electronics.

The PSB chamber is one four plane package identical to those used in PSA. It is located immediately downstream of RICH. The orientation of this package is Z,Y,Z′,Y′.

Both PSA and PSB are operated at 3.1 kV with a 50% argon, 50% ethane gas mixture bubbled through ethanol at 0°C. The amplifier and readout system is the same type as that used in the beam spectrometer. For unscattered beam muons, found using the beam spectrometer, the average single plane efficiency is estimated to be 90% for the subset of the 1987−88 data examined.

MUON DETECTION

Since the hadrons impinging on the 3.0 m thick iron wall interact and are absorbed, the basic signature identifying a muon is a track which continues downstream of the absorber.

High energy muons passing through matter often produce electromagnetic showers containing one or more electrons or positrons. These particles confuse the matching of tracks before and after a single absorber. In general the electromagnetic particles are low energy and can be absorbed in a few radiation lengths of material. The muon detection planes are therefore separated by 90 cm of concrete, which reduces the probability of track confusion and the chance that a beam muon will simulate a scattered muon in the trigger.

§*The SPM Scintillation Counters*

The SPM arrays are four planes of scintillation counters. Except for the central counters, each has dimensions 1.5 m×0.5 m×0.025 m; the central counters of each plane, above and below the beam, are 1.4 m×0.28 m×0.025 m. Counters in each plane are arranged, with 12 mm overlap, into walls with a total area of 3 m×7 m, see figure 6. The smaller scintillators are NE110† and are coupled to HAM R329 phototubes by an acrylic light guide for the upper counters and air guides for the lower (since these are in the beam).

† Nuclear Enterprises Ltd.

The scintillators shape and mounting leaves a hole 20 cm×20 cm, through which the beam passes. The larger counters are constructed of a single piece of 2.5 cm thick acrylic scintillator (ROHM GS2030) with wavelength shifter bars (ROHM GS1919) on each edge. The shifter bars are brought to a single photomultiplier tube (HAM R329). The bases for the counters have built-in integration and discrimination circuits. Discriminator outputs are transmitted over twisted pair cable to latches (LRS4448) and to the various trigger circuits for the experiment. In addition to the digital signals, the analog pulses are digitized (LRS2249) and read out for each counter. This permits monitoring of the response of the individual scintillators.

The phototube high voltages are supplied by LRSHV4032 modules and are monitored every thirty minutes.

§*The SMS Scintillation Counters*

The SMS counters provide fine resolution in, and close to, the beam. Each muon detection plane has two hodoscopes of scintillation counters which cover the hole in the SPM walls. SMSY1−4 are arrays of sixteen vertical counters each; SMSZ1−4 are the corresponding arrays of horizontal counters. The width of the counters is 13.2 mm, except for the outer ones, which are 19.6 mm. The scintillator is cut with beveled edges such that adjacent counters have an effective overlap of 0.3 mm. The phototubes (HAM R1166) are mounted directly on the scintillator, and the signals are taken to LRS4413 discriminators in update mode and to LRS2249 ADCs. Discriminator outputs go to LRS4448 latches and to the trigger logic. Phototube high voltages are supplied in the same way as the SPM counters.

§*The PTM Proportional Tubes*

Tracking in the muon detection system is done using 4 pairs of Y and Z view proportional wire tubes. The active area of the planes is 3.6 m×7.2 m. Each of the planes is constructed as a double layer of aluminum tubes of width 25.4 mm and wall thickness 2 mm. The two layers are displaced by 12.7 mm giving an effective wire pitch of 12.7 mm and no dead region between tubes (Figure 7). Usually a particle causes a wire hit in both layers.

The wires are 50 μm diameter gold plated tungsten and are operated at 2.7 kV. The gas mixture is 50% argon, 50% ethane bubbled through ethanol at 0°C, which gives a

maximum drift time for the electrons of 250 ns. Wire signals are amplified, discriminated and latched at the planes (NAN N-272-E). In addition the outputs from the monostables are available as ECL signals for use in the trigger electronics. Latch readout (NAN WCS 200 system) is done in parallel for each plane.

For muons in the halo, the typical efficiency for finding at least one PTM wire hit per station in single view is ~95% for the subset of the 1987–88 data examined. This measurement excluded a region around the beam.

§ *The RF Phase Locking System*

The Tevatron RF structure is preserved in the muon beam. During the 1987–88 running period the frequency was 53.10470 MHz. A signal source in the experimental hall is phase-locked to the arriving muons and used throughout the experiment; this PLRF signal has particular utility as a common time strobe since it has <1 ns time jitter relative to arriving muons.

The reference phase for the PLRF signal is provided by four 5.08 cm×5.08 cm×1.27 cm NE110 scintillation counters located downstream of the last SPM counter. Two RCA 8575 and two HAM R329 phototubes are used and the high voltages are supplied in the same manner as the SPM counters.

The counters are put in four fold coincidence; the output has a time jitter of 1.05 ns (FWHM) with respect to the accelerator RF. This signal is used to phase-lock the distributed accelerator RF, producing the PLRF signal. The phase-lock circuit can track time shifts at a rate of 300ps per arriving muon and has a back up local oscillator.

PARTICLE IDENTIFICATION

The design and construction of the following components of the Particle Identification system are influenced by the kinematic correlation between the momentum and production angles of particles produced in muon interactions. This correlation means, in general, that high momentum particles will be produced only at small angles in the laboratory. Low momentum particles, on the other hand, may be produced at large angles and are then further dispersed by the magnetic field of the CVM. The momentum ranges for pion, kaon and proton identification for each of the detectors, and their combined performance, is shown in Figure 8.

§*The TOF Time of Flight System*

The TOF system uses the same counter elements as were used in the NA9 experiment [5]; however the deployment of these counters and their operation has been considerably revised [15].

The scintillators are arranged in two hodoscope walls, each of which has thirty eight counters and covers a sensitive area of 4.2 m×1.6 m. Each counter is overlapped with its neighbors to ensure there is no gap in the acceptance. The counters vary in width (10 cm, 15 cm) and thickness (1.5 cm, 2 cm, 4 cm) across the walls. VAL† XP2020, XP2230, and XP2252 phototubes are employed. High voltage is supplied by LRSHV4032 modules. The TDCs are LRS2228 modules, and the pulse heights are digitized with LRS2249A ADCs.

A counter hodoscope is installed in the beam, just downstream of the first station of the beam spectrometer, to provide a precise measurement of the incident muon time [16]. This hodoscope has five scintillators with ten photomultipliers (VAL XP2252) arranged radially and designed to measure equal fractions of the muon beam (Figure 9). LRS2228, LRS2249A and LRSHV4032 modules are used for this hodoscope, as above.

A laser calibration system [17] is used to check stability. Ultraviolet light pulses (N_2 laser) are distributed by optical fibers directly into the scintillators where the UV light is shifted to blue. This accurately simulates the light produced by particles. The UV pulses arrive at the counters with a time spread less than 25ps; this simplifies the TOF calibration procedure. System stability and data integrity is checked frequently by a VME based dedicated processor. Twice per day UV pulses of variable intensity are used to track the pulse-height dependence of the time measurements.

Special calibration running is done once per data taking period to allow calibration of the TOF system, (Alignment and Calibration section). During the 1987–88 period the resolution for single particles was 320ps.

§*The C0 Threshold Cherenkov Counter*

The C0 Cherenkov counter was used in the NA9 experiment [5]. It consists of a radiator with an effective length of 90 cm and two mirror planes which reflect the light above and below the median plane of the detector into 144 Winston-Hinterberger cones. Each cone

† VAL: Valvo Hamburg.

focuses the Cherenkov light onto a phototube (16 RCA 8854Q, 128 EMI[†] 9829QA). Light from an individual particle may be collected by several phototubes, which are sensitive to single photoelectrons. The phototubes are shielded from the CCM and CVM fields by a composite shield built from a Mumetall[‡] tube, a soft iron housing, and bucking coils. The analog pulses are digitized using LRS2249A ADCs and discriminated with LRS4608Z modules. High voltage is supplied by LRSHV4032 units. The radiator gas is $C_2Cl_2F_4$ at atmospheric pressure, which has a refractive index of about 1.00141. The resulting Cherenkov thresholds for pions, kaons, and protons are 2.6 GeV/c, 9.3 GeV/c, and 17.6 GeV/c, respectively. The number of photoelectrons from a $\beta = 1$ particle is approximately fifteen. A subset of the phototubes are equipped with LRS2228 TDCs to record the pulse arrival time.

§*The C1 Threshold Cherenkov Counter*

C1 is an atmospheric pressure Cherenkov counter which was used in the NA9 experiment [5]. The radiator gas is a mixture of 70% nitrogen and 30% CCl_2F_2, which yields a refractive index of 1.00052. The Cherenkov thresholds for pions, kaons, and protons are 4.3 GeV/c, 15.3 GeV/c, and 31.0 GeV/c respectively. Its entrance window is 1.09 m×1.43 m, and the effective radiator length is about 1.5 m. The mirror arrangement focuses the Cherenkov light onto fifty eight phototubes (RCA 8854Q) which have 12.7 cm diameter photocathodes. The magnetic shielding for the phototubes uses three mu-metal tubes and a soft iron housing. The phototube pulses are digitized by LRS2249A ADCs and discriminated using LRS623BL discriminators; the times of arrival of the pulses are recorded using LRS2228 TDCs. The high voltages are supplied by LRSHV4032 modules. The number of photoelectrons for a $\beta = 1$ particle is measured to be approximately ten.

§*The RICH Ring Imaging Cherenkov Counter*

The RICH counter is described in detail elsewhere [18,19]. The detector consists of a 6 m long radiator vessel; thirty three spherical mirrors, of the Omega design [20], covering an active area of 2.7 m×3.7 m; and a photon detector with a 40 cm×80 cm active area (Figure 10). The mirrors have an average focal length of 4.85 m and are aligned on a common sphere. The Cherenkov light reflected from the mirrors is imaged into rings at

[†] EMI: EMI corporation

[‡] Vakuumschmelze GmbH Hanau

the focal plane where the photon detector is mounted. The photon detector consists of a calcium fluoride window followed by a drift space and a MWPC filled with 99.3% methane and 0.7% triethylamine (TEA).

The proportional chamber is made up of a cathode wire plane constructed from 50 μm diameter copper beryllium wires on a 500 μm pitch; an anode plane of 20 μm gold plated tungsten wires with 2 mm spacing; and a second cathode plane which is an array of 10800 pads, each 3.8 mm$\times$12 mm, read out individually. Analog zero-suppression is performed and only signals above a pre-set threshold are digitized for readout. The anode wires are read out using a similar scheme.

The choice of gas for the radiator volume is based on a balance between the number of photons needed to ensure good pattern recognition and the momentum range of particle identification that can be achieved. During the 1987–88 data taking period most of the running was done with pure argon in the radiator. This choice resulted in approximately 5.4 detected photons per ring and a measured spatial resolution of 2.5–3 mm, which is comparable to that expected from chromatic aberration. Under these conditions, three sigma π/K separation up to particle momenta of 100 GeV/c is possible. ,

ELECTROMAGNETIC CALORIMETRY

The electromagnetic calorimeter (Figure 11) is described in detail elsewhere [21]. The calorimeter has twenty planes of one radiation length thick lead interspersed with twenty wire chamber planes. The active area is 3 m$\times$3 m. Wires are 50 μm and 63 μm diameter Cu-Be, 1.04 cm apart on average, and are read out in groups of sixteen adjacent wires. In the four planes closest to the shower maximum, wires are read out individually in the central 1 m of the detector and in pairs in the outer regions. The chambers have alternately Y and Z wires in consecutive planes. The cathode planes are split into 1188 pads, and read out as towers summed over all planes. The pad size is 4 cm$\times$4 cm in the central 1 m$\times$1 m of the detector, 8 cm$\times$8 cm between 0.5 m and 1 m from the beam, and 16 cm$\times$16 cm in the outer region of the detector. The readout is via FASTBUS using LRS1821s and LRS1892s with LRS1885 ADCs. The spatial resolution for isolated particles is $\sim$5 mm using the pad information and $\sim$3 mm using the wire information. Two photons in the central part of the detector can be resolved if they are separated by more than $\sim$12 cm, using pad information. Energy depositions with two centers can be identified using the

wires down to a separation of 4 cm, which corresponds to the minimum photon separation for an 80 GeV π^0. Based on the π^0 peak and electron beam test data, the energy resolution is $\sim 7\% + 45\%/\sqrt{E}$ where E is the photon energy in GeV. This is worse than the resolution expected from prototype tests, but final corrections for various effects, such as gas-gain and position dependence have not yet been implemented.

The chambers are operated at 2.0 kV and 2.15 kV, in proportional mode, with 50% argon and 50% ethane as the gas. After mixing, the gas is flowed through a buffer tank with twenty times the volume of the calorimeter; this ensures that the argon content in the mixture changes at a rate less than 0.2%/day. The gas gain is continuously monitored with small single wire proportional chambers that contain ^{55}Fe sources. The pulse-height spectra from these chambers are recorded between spills during data taking, and allow the gas gain to be monitored to 1%. Halo muons are also used to track the gas gain.

TRIGGERS

The apparatus is normally operated with a mixture of different triggers. Physics, calibration, and monitoring triggers are run simultaneously during data taking. For short periods some of these triggers are slightly modified for use in the electron beam mode and for alignment running. In this section we outline the motivation and implementation of those triggers used during the 1987–88 data taking run.

The ideal physics trigger for this experiment would select deep-inelastic events on the basis of Q^2 and ν, where Q^2 is the virtual photon mass squared and $\nu = E - E'$ (E incident muon energy, E' scattered muon energy). The experiment trigger is based on the difference in direction between the muon going into the target and the muon leaving the target. For deep-inelastic events this scattering angle, θ_{scat}, is given by

$$Q^2 = 4EE'sin^2(\theta_{scat}/2)$$

so that a trigger based on the scattering angle accepts events on the basis of a combination of both Q^2 and ν. In practice, an angle cut approximates a Q^2 cut when integrated over the range of ν accepted by the trigger.

Since the muon beam energy is twice that of earlier experiments, a natural goal of this experiment is the study of low x_{bj} events ($x_{bj} = Q^2/(2m_p\nu)$, where m_p is the mass of the proton). This is because, for a given Q^2, $(x_{bj})_{min} \propto 1/(E - E')$. For a fixed beam energy,

$(x_{bj})_{min} \propto Q^2$, so that it is necessary to collect low Q^2 data and, therefore, trigger on low scattering angle events, see Figure 12. At low angles, the interaction can leave the scattered muon inside the phase space of the muon beam and a number of background processes become more serious. To overcome these problems, a separate trigger is used for small angle scattering. During the 1987–88 run the small angle trigger used 12% of the muon beam defined for use at higher angles of scatter.

The trigger logic for the experiment is arranged in two levels. This structure allows trigger decisions to be made on a more sophisticated basis. Level-1 triggers generate the gates and strobes for most of the equipment; wire chamber data and integrated analog signals are available at level-2. Readout does not proceed until a level-2 trigger is generated. If a level-2 trigger does not occur in association with the level-1 the apparatus is cleared without readout. On average the deadtime incurred as a result of a level-1 trigger without a subsequent level-2 is 2-3 μs. Readout of the apparatus takes 2-3 ms. These times limit the level-1 trigger rate to 40k s^{-1} ($\sim$10% deadtime) and the level-2 rate to 80 s^{-1} ($\sim$20% deadtime). During the 1987–88 data taking period level-2 conditions were used only for triggers related to the streamer chamber. The experiment typically operated with 80% livetime.

Table 4 lists the salient features of the ten triggers used during the 1987–88 data taking period.

The optics of the spectrometer is arranged to simplify the trigger. The field directions of the CVM and CCM are opposite. Their field integrals are inversely proportional to their distance from the first plane of the PTMs and are 4.315 Tm and -6.734 Tm respectively. Neglecting various achromatic effects, the result of this focussing condition is that the impact position at PTM1 for a scattered muon depends only on the scattering direction and not on the muon energy. Behind PTM1 the divergence of muon trajectories, from this point, is determined by multiple scattering and the scattered muon energies. Focussing also ensures that unscattered beam muons hit the SMS1 arrays at the position predicted by a straight line projection from the beam spectrometer, independent of energy. This is crucial to the operation of the the small angle trigger. Since the target is inside the CVM, scattered muons change momentum part way through the CVM field; this is the major achromatic effect and is one of the limitations on the small angle trigger performance.

§*The LATB and SATB Beam Definitions*

One component of most physics triggers is a signal that indicates a beam muon has entered the target in an acceptable direction. The definition of a beam muon depends on the physics trigger being considered.

For large angle scatters, a beam muon, LATB, is defined as a hit in all seven of the SBT hodoscopes in coincidence with the PLRF signal (RF Phase Locking section) and in anti-coincidence with the OR of the counters in the SVJ and SVW hodoscopes. The halo system vetoed three RF buckets: the one that contained the muon that hit the wall and the buckets either side of it. The SVJ and SVW conditions excluded 10-20% of the muons which satisfied the seven fold SBT coincidence. Some of the scintillators in the SBT hodoscopes were excluded from the beam definition as a result of tuning the large angle scatter trigger.

A second beam definition, used by the small angle trigger, is required because muons scattered at small angles can remain inside the region of the overall beam. In order to detect such scatters, the incoming muon directions must be either restricted, or measured. The small angle trigger beam, SATB, is defined as a subset of the muons for which the incoming direction is measured using the highest resolution central SBT counter region. The signals from the SBT scintillators are routed to an ECL based look-up table, which is loaded with acceptable scintillator combinations; those that satisfy an allowed combination produce an SATB signal. An additional requirement, implemented for a subset of the data taking during the 1987–88 data taking period, was that there be no muon in the RF bucket either side of the one used and that there be no extra hits in the SBT arrays. All triggers made using the SATB have the PLRF signal as an additional component.

§*The LAT Large Angle Trigger*

Most of the LAT trigger rejection is provided by a veto condition, which detects unscattered muons and discards events rather than detecting scattered muons and triggering. It is the veto component of the LAT which makes it effective as a trigger for the experiment.

The divergence of the beam used by this trigger, LATB, as defined above, is such that unscattered muons hit the SMS hodoscopes behind the absorber. The LAT is formed as LATB in coincidence with hits in three out of four of the SPM scintillator planes behind the steel hadron absorber, and in anticoincidence with the OR of the counters in the SMS

hodoscope directly behind the absorber and those in the SMS hodoscope behind the last concrete wall (both Y and Z views). The individual counters in each SPM plane are ORed for use in the three out of four coincidence. For muons centered on the SMS array, this is a 3.3-4.7 mr angle cut; for 500 GeV/c incident muons, at $E = E'$, this corresponds to Q^2 =2.7 GeV^2/c^2−5.5 GeV^2/c^2. Figure 12 shows the acceptance as a function of Q^2 and x_{bj}.

§*The SAT Small Angle Trigger*

The SAT also works as a veto. Only muons which point towards the center of the SMS arrays are considered. For each of the SATB muons the impact point in the SMS arrays is calculated using the SBT counters. A veto region, a minimum of three SMS counters wide in both the Y and Z views, is dynamically defined and used to veto the beam. An ECL based hardware look-up table is used so that this dynamic vetoing can be done for each RF bucket. The SAT trigger was used in various configurations during the 1987−88 run; most data was taken without an SPM or SMS hit requirement and with the veto in the Y view only. This configuration results in overlap between the SAT and the LAT which is useful for checking trigger efficiencies. The effective angle cut was ∼1 mr, with high efficiency and well defined acceptance at $E = E'$ for 500 GeV/c muons down to a Q^2 of 0.5 GeV^2/c^2. Figure 12 shows the Q^2 and x_{bj} dependence of the SAT trigger. The SAT trigger is formed as a coincidence between SATB and the PLRF signal, vetoed by the the dynamic veto.

§*The LATRBEAM and SATRBEAM Normalization Triggers*

One component necessary to normalize the data is the number of muons which pass through the detector during its livetime and which can be reconstructed offline. The "random beam" method [22] is used as the primary normalization measurement. This method works particularly well at the Tevatron muon beam because the muons are located at 19 ns intervals to a precision of 1 ns. RF buckets are selected at random using a random number generator [23] synchronized to the RF. If there is a beam signal associated with the selected bucket the experiment is triggered. This trigger is used concurrently with the trigger it is intended to normalize, which ensures that the livetime is correctly sampled. The rate of random selection and the fraction of such triggers which yield a reconstructible beam muon offline give an accurate determination of the muon flux used for all triggers that

use the beam signal as a component. There must be one such "random beam", RBEAM, trigger for each different beam definition formed. During the 1987–88 run there were two beams and two random beam triggers; one associated with the LAT trigger, LATRBEAM, and one for the SAT trigger, SATRBEAM. The random bucket selection rate is tuned such that the number of LATRBEAM and SATRBEAM triggers is about 10% of the triggers they are normalizing. This ensures that 1% statistical precision in normalization can be achieved over a period of six hours during typical running.

§*The FCAL Electromagnetic Energy Trigger*

In addition to muon flux, normalization of physics triggers requires that the efficiency of the scattered muon detection and offline reconstruction be understood. There is overlap between the SAT and LAT triggers, but both depend on the scintillator arrays behind the steel absorber. In order to have an independent trigger for studies of systematic effects, a trigger based on the electromagnetic calorimeter is used. Subject to the biases inherent in triggering predominantly on the electromagnetic energy, this trigger can also be used to study events outside the kinematic regions accessible to the other triggers. The total energy in the calorimeter, excluding a 32 cm wide cross centered on the beam, is formed and discriminated. This is put into coincidence with the PLRF signal and a subset of the LATB beam. The central region has to be excluded to prevent various electromagnetic processes from swamping the deep inelastic trigger rate. Since the calorimeter is a wire-chamber device with a long response time, incident muons are only considered if there is no muon in the preceeding fifteen buckets. The energy threshold during the 1987–88 run was approximately 60 GeV/c.

§*The HALO Halo Trigger*

For continuous monitoring of chamber alignment and efficiency and for diagnostic purposes, a trigger is used which detects the halo muons. Since these are outside of the normal beam phase space and are spread out over the whole of the apparatus, they are valuable as a monitoring tool. In order to trigger on these muons a coincidence is formed between the upstream veto wall (SVJ, SVW), the phase-locked beam RF and three out of four of the SPM planes downstream of the absorber. This trigger is prescaled so that during normal data taking it typically represents 5% of the trigger rate (50/spill).

§The PCLAT and pre-scaled (PCSAT,SAT,LAT) Streamer Chamber Triggers

As discussed earlier, the typical rate at which the streamer chamber can take pictures is about 1.5 s^{-1}. The electronic apparatus can take data at 80 s^{-1} so that only a fraction of the electronic events can have streamer chamber information. Neither of the two physics triggers used during the 1987–88 data taking (LAT, SAT) have a rate compatible with the streamer chamber, so a level-2 restriction was used to enhance the fraction of electronic triggers that were real events.

The primary streamer chamber trigger, PCLAT, was a copy of the LAT trigger with a level-2 requirement based on three Z planes of the PC chambers. Majority logic modules (LRS4532s) were used to select events which had at least two wires hit anywhere in the three planes. Hits in a vertical stripe 19.2 cm wide were excluded from consideration to eliminate beam related effects. 20–40% of the PCLAT triggers were deep inelastic events. Monte-Carlo studies indicate that this requirement introduces little bias for events with $\nu > 40$ GeV and $Q^2 > 10$ GeV$^2/c^2$.

In addition to the PCLAT trigger, the SAT analog was formed, PCSAT, and used as a streamer chamber trigger. Finally, the LAT and SAT triggers were prescaled and used to trigger the streamer chamber. This was done to help understand potential biases introduced by the PC requirement.

READOUT AND ONLINE MONITORING

The overall apparatus data acquisition system is shown in Figure 13. The main interface is CAMAC with six CAMAC branches attached to three front-end PDP11/34s† [15,24]. There is one serial CAMAC branch, used to acquire data not read each event and for control functions. In addition a FASTBUS system acts as a fourth front end. The front-end machines read out in parallel, in 2–3 ms, and the data is stored in bulk memory on the PDP UNIBUS and in LRS1892 memory modules. Asynchronously, a μVAX II* reads the buffered information over DR11W links, concatenates data from the front-ends into single events, and writes the information onto 6250bpi tapes. The μVAX also sends a sample of the concatenated events to a VAX–11/780† for real-time analysis and monitoring. The system is capable of acquiring and logging data at an averaged rate of 250 kbytes/s; the

† Digital Equipment Corporation

typical event size is 10 kbytes. Consequently, the maximum rate during the 20 s muon beam pulse is 750 kbytes/s. Since the data logging is asynchronous, the apparatus deadtime depends only on the ~3 ms readout time; at the maximum throughput the apparatus deadtime from readout is ~20%.

The framework of the data acquisition is the FNAL VAXONLINE system [25] and RSX-DA [26]. These packages form the software basis for communication, concatenation, data logging, run control, message distribution, and online event handling.

Four kinds of online monitoring are performed: front end monitoring of basic hardware operation and periodic calibration; general checks of the data structure integrity after concatenation; online analysis of individual detector systems (wiremaps for example); and immediate readback and analysis of a subset of the raw data tapes.

During the periods between muon pulses, monitoring tasks run on the front end PDP11/34s and on several stand alone microprocessor systems. These tasks create and format calibration and diagnostic information into events that are incorporated into the data stream and logged to tape. Among others, tasks are run which: flash scintillator LEDs; pulse chamber wires; check HV, CAMAC and NIM crate voltages; confirm trigger processor RAM contents; calibrate ADCs and TDCs; and measure temperatures. In the case of abnormal conditions error messages are issued. These messages are collected, logged, and displayed by a central message facility on the VAX−11/780. Tasks of this kind monitor the basic hardware functions at all times during data taking.

Concatenated events are shipped to the online VAX−11/780 continuously during data taking. Several monitoring programs analyze various aspects of the events. The raw event structure is continuously monitored as a basic check of the data acquisition system integrity. Data from individual detectors are also analyzed and key distributions are checked frequently by shift personnel. Online event displays provide additional, important, diagnostic information regarding the state of the apparatus.

Approximately once every two hours during data taking a raw data tape is transferred to a local μVAX and analyzed with the offline software. This is a final check that the whole data aquisition chain is functioning correctly.

CALIBRATION and ALIGNMENT

The individual detectors are nominally installed in predefined positions in the E665 reference frame and are optically surveyed in place. An improved determination of position is obtained by analysis of data from HALO and RBEAM triggers taken during special runs with various combinations of the spectrometer magnets on and off. A summary of the special alignment conditions used during the 1987–88 data taking period is given in Table 5 along with their primary purpose.

Day to day variations in the position of the beam and spectrometer wire chambers can be monitored with the sample of RBEAM and HALO triggers which constitute an integral part of the data stream.

The halo and beam muons do not provide particles with the appropriate trajectories or identity to calibrate the particle identification detectors or the calorimeter. The Cherenkov counters require $\beta = 1$ particles coming from the target region at large angles. The TOF counters require particles with $\beta = 1$ and well defined path lengths. The electromagnetic calorimeter requires either electrons or photons of known energy over as much of the face of the calorimeter as possible. In order to satisfy these requirements a tertiary electron beam is generated, as described in the section on the beam. This beam is operated over a momentum range of 2 GeV/c - 150 GeV/c; by adjustment of the spectrometer magnets and the rotating dipole in the beamline, a large fraction of the total detector surfaces are illuminated. Some results of the calibration running performed during the 1987–88 run have already been mentioned in conjunction with the relevant detectors.

DETECTOR UPGRADES

Several upgrades to the apparatus are planned for the next Tevatron fixed target running period. These changes are motivated in part by the specific physics program to be addressed in the run and in part to improve the experiment trigger, in terms of both bias and rejection. The modifications are outlined here for the sake of completeness and will be described in detail in a future publication.

For most data taking the target location will be upstream of the CVM and will be a rotating set of both heavy targets and hydrogen and deuterium. Several planes of small cell drift chambers will be located in the CVM aperture to replace SC and improve vertex resolution. A low mass proportional wire chamber package of similar design to PSA will

replace PSB and be located just upstream of the DC1-4 package; a second set of these chambers will be mounted in the field of the CVM as part of the drift chamber vertex system.

Two walls of scintillation counters, each with an effective area of 7 m×3 m and a beam hole, will be located upstream of the hadron absorber (and CAL in the central region). The scintillation counters will be arranged to cover the acceptance of the SPM walls and will be used as part of the wide angle trigger level−1 logic. Additionally the central counters in each SPM plane will be upgraded to have single RF bucket time resolution and to allow an adjustable hole size for the beam. Trigger electronics that finds PTM wire chamber track projections will be used at level−2. A hodoscope of scintillation counters will be mounted, centered on the beam, in a hollow in the downstream side of the steel absorber. The array will be of adjustable size, up to 22 cm×31 cm, and will be used as a veto element in the wide angle trigger logic.

The level−1 SAT trigger will be upgraded to use 70% of the LAT beam and a small angle veto based on PSA wires will be employed at level−2. The wire hits will be masked by an array of finger counters, similar to the SMS arrays, covering 13 cm×13 cm in the beam region just upstream of CAL.

CONCLUSIONS

The elements and operation of the large spectrometer used by the E665 collaboration have been described. The information presented in this paper shows that there are already many indications that the apparatus is working well.

ACKNOWLEDGEMENTS

The support of FNAL during the construction and commissioning of the apparatus was indispensable. The detector could not have been built without the expert services of many of the FNAL support divisions.

Many people not on the author list made major contributions to the construction and design of the apparatus, all cannot be cited individually. Of particular value was assistance rendered by:

S. Austin, E. Beck, H. Bruch, C. Danner, R. Denham, G. Duckett, Y. Etchavaria, E. Frazier, D. Goloskie, P. Gorak, T. Griffin, J. Guerra, S. Harrold, D. Hicks, J. Hurley, R. Jones, K. Kephart, J. Korienek, B. LaVoy, J. MacNerland, A. Malensek, T. May, W. Newby, J. O'Connell, D. Petravick, R. Pordes, S. Pordes, T. Regan, J. Sasek, J. Schellpfeffer, and S. Strecker from FNAL.

A. White from the University of California, San Diego.

U. Seidler from the University of Freiburg i.Br.

J. Blandino, J. McElaney and J. Oliver from Harvard.

D. Northacker from the Max Planck Institute for Physics & Astrophysics.

W. Francis, R. Pitt and A. Weidemann participated in the early stages of the experiment.

The work of the University of California, San Diego was supported in part by the National Science Foundation, contract numbers PHY82-05900, PHY85-11584 and PHY88-10221; the University of Illinois at Chicago by NSF contract PHY88-11164; and the University of Washington by NSF contract numbers PHY83-13347 and PHY86-13003. The University of Washington was also supported in part by the U.S. Department of Energy, as were Harvard University; the University of Maryland, College Park; the Massachusetts Institute of Technology; and Yale University. The University of Freiburg i.Br. and the University of Wuppertal were supported in part by the Bundesministerium fuer Forschung und Technologie.

The University of Maryland group wishes to thank I.N.F.N. Frascati, and CERN, for the use of facilities during construction of chambers for CAL.

REFERENCES

[1] Francis W.R., and Kirk T.B.W, Physics Reports 54C (1979) 307

[2] Drees J., and Montgomery H.E., Ann. Rev. Nucl. and Part. Sci. 33 (1983) 383

[3] Nowak W.D., Fortschritte der Physik 34 (1986) 2,57

[4] Sloan S., and Voss R., Smadja G., Physics Reports 162C (1988) 45

[5] Albanese et al., Nucl Instr. 212 (1983) 111

[6] Malensek A., and Morfin J., FNAL TM-1193, 1983

[7] Conrad J.M., Malensek A., Morfin J., FNAL TM in preparation

[8] Fenker H., FNAL TM-1179 1983

[9] Gebauer H.J., E665 Internal Report, VS012 MU001 1986

[10] De Palma M., et al., Nucl. Instr. 217 (1983) 135

[11] Lindsay J.B., et al., Nucl. Instr. 156 (1978) 329

[12] Bhatti A. et al., E665 Internal Report, UW016 FS011 1986

[13] Kirk T., Melanson H., Wolbers S., E665 Internal Report, FL027 FS010 1985

[14] Kirk T., E665 Internal Report, FS017, 1978

[15] Erdmann M., E665 Internal Report, FR001 VS015, 1986

[16] Wilhelm M., Diploma Thesis, Univ. Freiburg i.Br., July 1988

[17] Erdmann M., Diploma Thesis, Univ. Freiburg i.Br., November 1985

[18] Coutrakon G.B., et al., IEEE Trans. Nucl. Sc. NS-35 (1988) 470

[19] Dhawan S.K., et al., IEEE Trans. Nucl. Sc. NS-35 (1988) 436

[20] Apsimon R.J. et al., RAL-85-014, June 1985

[21] Aid S., et al., 1985 FNAL Gas Sampling Calorimetry Workshop, P249

[22] Mount R.P., Nucl. Instr. 187 (1979) 23

[23] Hill W., Horowitz P., Cambridge Univ. Press, Cambridge 1980

[24] Geesaman D.F., et al., Summary submitted to the Sixth IEEE Real-Time Conference, May 15-18 1988, Williamsburg, VA

[25] Berman E., et al. IEEE Trans. Nucl. Sc., NS-34 (1987) 763

[26] Berg D.M., et al. IEEE Trans. Nucl. Sc., NS-32 (1985) 1368

TABLE CAPTIONS

Table 1 Summary of Detector Parameters.

Table 2 Beam Performance Parameters. (See text for detailed definitions).

Table 3 1987–88 Targets.

Table 4 Trigger Parameters.

Table 5 Alignment Running Conditions.

FIGURE CAPTIONS

Fig. 1 A view of the main elements of the NM beamline, including the beam spectrometer.

Fig. 2 Plan and perspective views of the E665 spectrometer.

Fig. 3 Muon beam profile at the target, projected from the beam spectrometer, neglecting the CVM field, and using RBEAM triggers.

Fig. 4 Beam tagging station, including SVJ counters.

Fig. 5 A streamer chamber picture.

Fig. 6 SPM array.

Fig. 7 PTM tube plane wire offset arrangement.

Fig. 8 Particle identification of the combined PID detectors.

Fig. 9 TOF start counter arrangement.

Fig. 10 RICH counter construction.

Fig. 11 CAL cathode pad layout.

Fig. 12 Q^2 and Y acceptance of the SAT and LAT triggers. At the trigger level the SAT does not require a muon in the muon detection system, which accounts for the difference between the LAT and SAT trigger acceptance at high Q^2 and Y.

Fig. 13 Data acquisition system.

Table 1

Chamber Devices						
Detector Name	Detector Type	Active Area (m)	Number of Planes	Wire Spacing or Resolution	Active Gas † (mg/cm^2)	Total Material (g/cm^2)
PBT	prop. wire	0.13 x 0.13	4 x (U;Z;Y;V;Z';Y')	1 mm	0.7	–
SC	streamer ch.	2.0 x 1.2 x 0.7	–	850 μm	–	–
PCV	prop. wire	2.8 x 1.0	Y;U;U';V;V';Y	2 mm	2.2	0.49
PTA	prop. tube	2.0 x 2.0	Y;Z;V;U	7.2 mm	5.1	–
PC	prop. wire	2.0 x 2.0	3 x (Y;Z;V;U)	3 mm	1.4	.33
PCF	prop. wire	2.0 x 1.0	5 x (U;V;Z)	2 mm	1.3	2.5
DC1-4	drift ch.	2.0 x 4.0	4Z;2U;2V	<400 μm	1.0	0.05
DC5-8	drift ch.	2.0 x 6.0	4Z;2U;2V	<400 μm	1.0	0.05
PSA	prop. wire	0.13 x 0.13	Z;Y;Z';Y';U;V;U';V'	1mm	0.7	–
PSB	prop. wire	0.13 x 0.13	Z;Y;Z';Y'	1mm	0.7	–
PTM	prop. tube	3.6 x 7.2	4 x (Y;Z)	12.7 mm	5.1	–

Scintillation Hodoscopes					
Detector Name	Material	Thickness (cm)	Array Size (m)	Number of Elements	Photomultiplier
SBT	NE110	1.0	0.18 x 0.13	4 x [26, 13Y;13Z]	R1398
SVJ	NE110	1.0	0.5 x 0.5	3 x 2 [with hole]	RCA8575
SVW	NE110	1.0	7.0 x 3.0	28 [14 x 2 array]	RCA8575
TOF	NE110	1.5,2.0,4.0	4.2 x 1.6	2 x 38	XP2020,XP2230,XP2252
	NE104	1.0	0.2 x 0.2	5 [radial]	XP2252
SPM	GS2030	2.5	7.0 x 3.0	4 x 30 [15 x 2 arrays]	R329
SMS	NE110	1.0	0.2 x 0.2	4 x 32 [16Y,16Z]	R329

Cherenkov Detectors							
Detector Name	Index of Refraction	Radiator Length (m)	Number of Cells	Detector/ Photomultiplier	Thresholds (GeV/c)		
					π	K	p
C0	1.00141	0.9	144	RCA8854Q,EMI9829QA	2.6	9.3	17.6
C1	1.00052	1.5	58	RCA8854Q	4.3	15.3	31.0
RICH	1.00033	6.0	10800	wire chamber	5.4	19.2	36.5

Electromagnetic Calorimeter						
Detector Name	Detector Type	Active Area (m)	Number of Planes	Number of Cathode Towers	Wire Spacing	Total Thickness (radiation lengths)
CAL	gas sampling	3.0 x 3.0	10 x (Y:Z)	1188	1.04 cm	20

† Active gas thickness per wire chamber plane.

Table 2

Nominal Energy Tune	<momentum> LATRBEAM Trigger	Momentum spread (sigma)	LATB/P measured (typical)	LATB/B measured (typical)	HALO/LATB (typical)
500 GeV	486 GeV/c	60 GeV/c	$.55\times10^{-5}$	.88	.20
100 GeV	109 GeV/c	23 GeV/c	$.97\times10^{-5}$	.81	.37

B = 7/7 SBT
LATB = 7/7 SBT . NOT(SVW + SVJ) – Large angle trigger beam
HALO = (SVJ1 . SVJ2 . SVJ3) + (3/4 SPM. SVW. NOT(CVJ))
P = number of protons on Be target (Tevatron total $\sim 10^{13}$/minute)

Table 3

Target	Energy (GeV)	Density (g/cm^3)	Error [a] stat. %	Error [a] syst. %	Pressure (kPa)	Temperature (K)
H_2	500	0.07070	0.01	0.07	103.5 [b]	20.3
D_2	100	0.1626	0.009	0.3	104.6 [b]	23.8
D_2	500	0.1626	0.005	0.3	104.8 [b]	23.8
Xe	500 & 100	0.0853	0.2	0.2	1448 [c]	293 [c]
Xe	500	0.04090	0.04	0.3	717 [c]	293 [c]
He [d]	500	0.00017	1.0	2.0	103 [c]	293 [c]

[a] Preliminary Errors on Density
[b] Vapor Pressure
[c] Approximate
[d] Empty Target Data

Table 4

Trigger	Beam	Halo [c] Veto	Scattered Muon	Back [d] Veto	Other Req.	Prescale Factor	Triggers/ LATB [a]
LAT	7/7 SBT	SVW+SVJ	3/4 SPM	SMS1 +SMS4	–	1	2×10^{-5}
SAT	Roads in SBT Y and Z	Muon in neighbor buckets	–	0.06 m region in SMS	–	1	2×10^{-5}
PCLAT [b]	7/7 SBT	SVW+SVJ	3/4 SPM	SMS1 +SMS4	hits in PCN	1	3×10^{-6}
PCSAT [b]	Roads in SBT Y and Z	Muon in neighbor buckets	–	0.06 m region in SMS	hits in PCN	1	1×10^{-6}
LAT [b]	7/7 SBT	SVW+SVJ	3/4 SPM	SMS1 +SMS4	–	2^4	1×10^{-6}
SAT [b]	Roads in SBT Y and Z	Muon in neighbor buckets	–	0.06 m region in SMS	–	2^6	3×10^{-7}
LAT-RBEAM	7/7 SBT	SVW+SVJ	–	–	random prescale	2^{19}	2×10^{-6}
SAT-RBEAM	Roads in SBT Y and Z	Muon in neighbor buckets	–	–	random prescale	2^{16}	3×10^{-6}
FCAL	7/7 SBT	SVW+SVJ +(muon in 5 bkt)	–	–	Energy in CAL	1	1×10^{-5}
HALO	(SVW+SVJ) .3/4 SPM	–	–	–	–	2^{10}	7×10^{-6}

All trigger rates are defined relative to the LATB, including the SAT triggers which use a subset of LATB (see the LATB and SATB sections in text)

[a] Typical values for 500 GeV muons on H_2.

[b] Streamer Chamber Triggers

[c] Veto conditions applied to beam definition

[d] Veto used downstream of hadron absorber

Table 5

Tagging Magnet	CVM	CCM	Trigger	Primary function of the data
off	on	on	HALO	To obtain the relative alignment of the beam spectrometer and the chambers in the forward spectrometer
off	on	off	7/7 SBT	
off	off	off	HALO	
off	off	off	7/7 SBT	
on	off	off	HALO	To obtain the relative alignment of the chambers in the forward spectrometer
on	off	off	7/7 SBT	
on	off	off	HALO (w/o SVJ)	
on	off	off	LAT (w/o SPM)	
on	on	on	HALO (w/o SVJ)	To locate the DC dead regions accurately and to map drift velocity corrections
on	on	off	HALO	
on	on	off	HALO (w/o SVJ)	

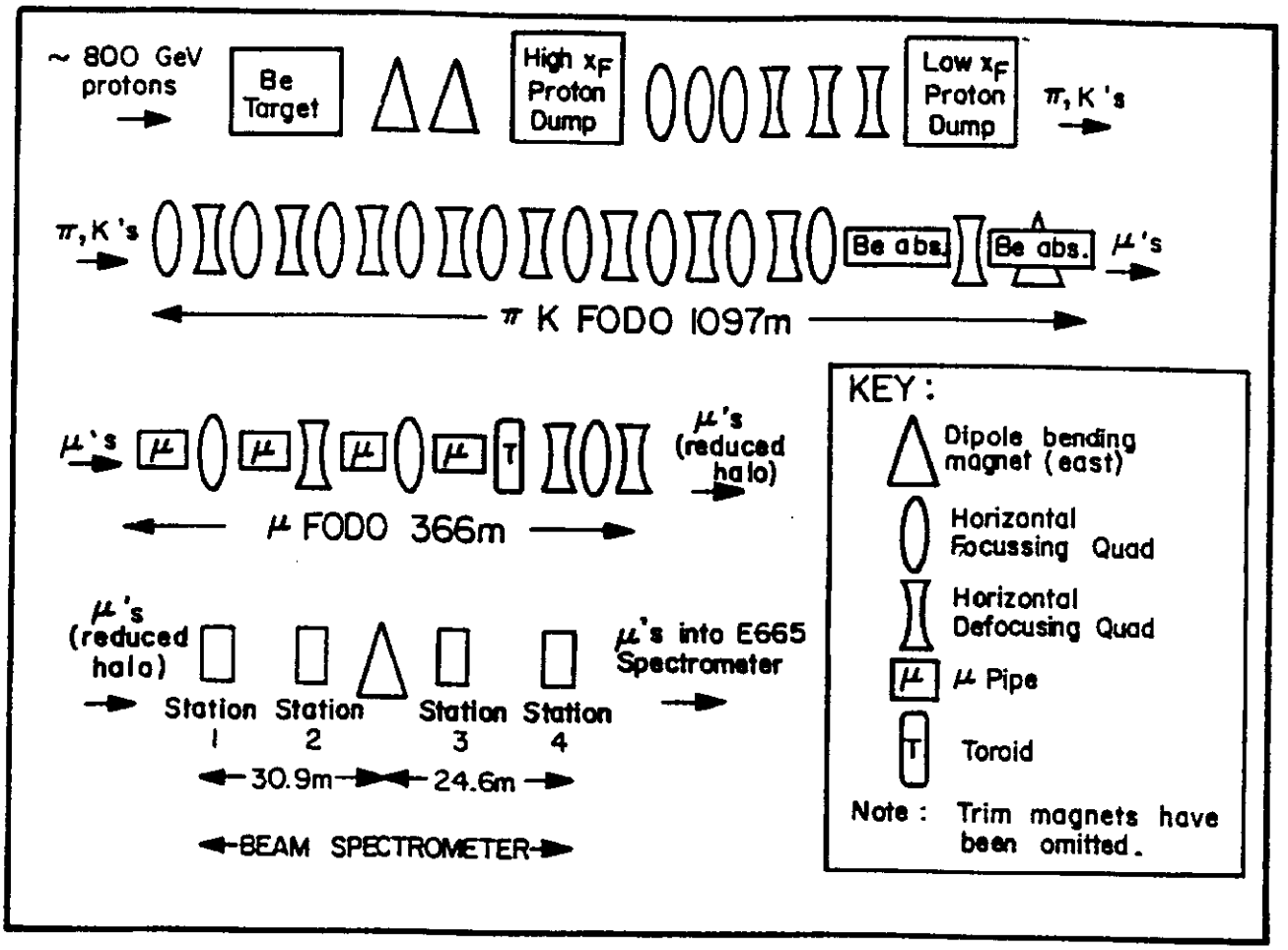
~ 800 GeV protons
Be Target
High x_F Proton Dump
Low x_F Proton Dump
π, K 's
π,K 's
Be abs.
Be abs.
μ's
π K FODO 1097m
μ's
μ's (reduced halo)
μ FODO 366m
μ's (reduced halo)
μ's into E665 Spectrometer
Station 1
Station 2
Station 3
Station 4
30.9m
24.6m
BEAM SPECTROMETER
KEY :
Dipole bending magnet (east)
Horizontal Focussing Quad
Horizontal Defocusing Quad
μ Pipe
T
Toroid
Note : Trim magnets have been omitted.

Figure 1

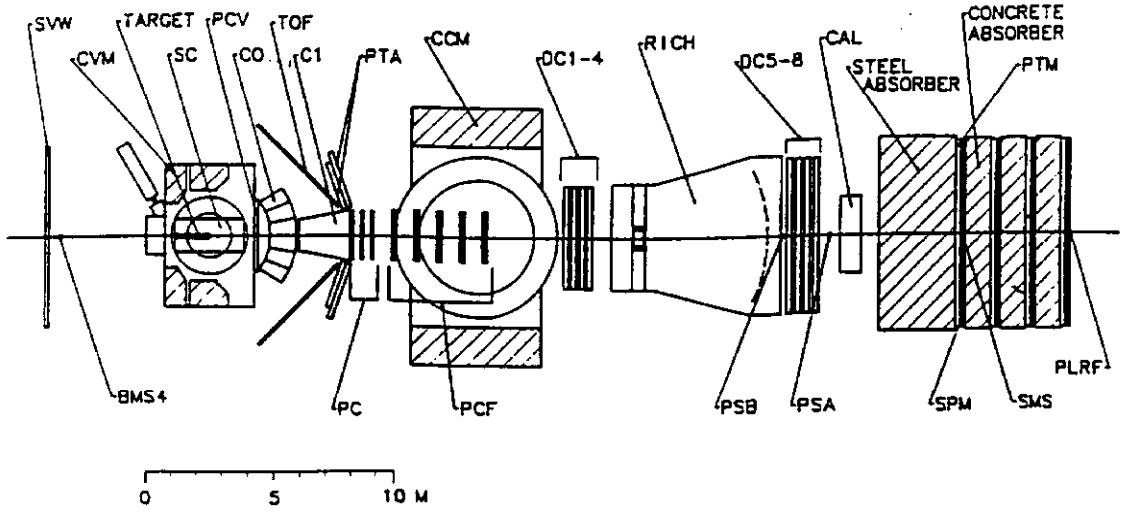
SVW
TARGET
PCV
TOF
CVM
SC
CO
C1
PTA
CCM
DC1-4
RICH
DC5-8
CAL
CONCRETE ABSORBER
STEEL ABSORBER
PTM
BMS4
PC
PCF
PSB
PSA
SPM
SMS
PLRF
0
5
10 M

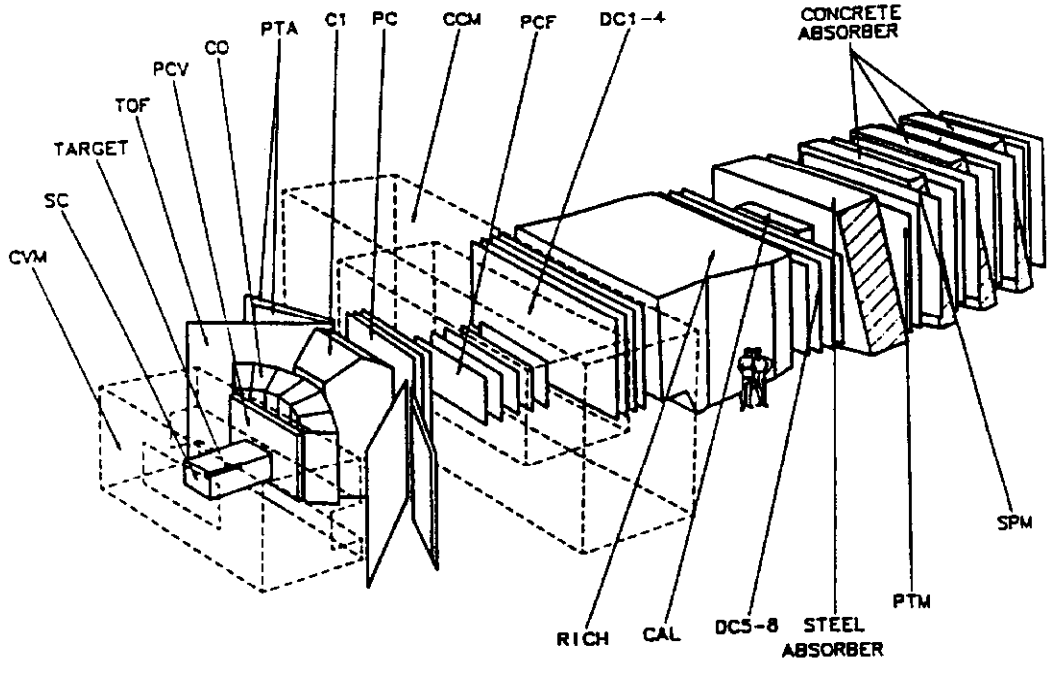
PTA
C1
PC
CCM
PCF
DC1-4
CONCRETE ABSORBER
CO
PCV
TOF
TARGET
SC
CVM
SPM
PTM
RICH
CAL
DC5-8
STEEL ABSORBER

Figure 2

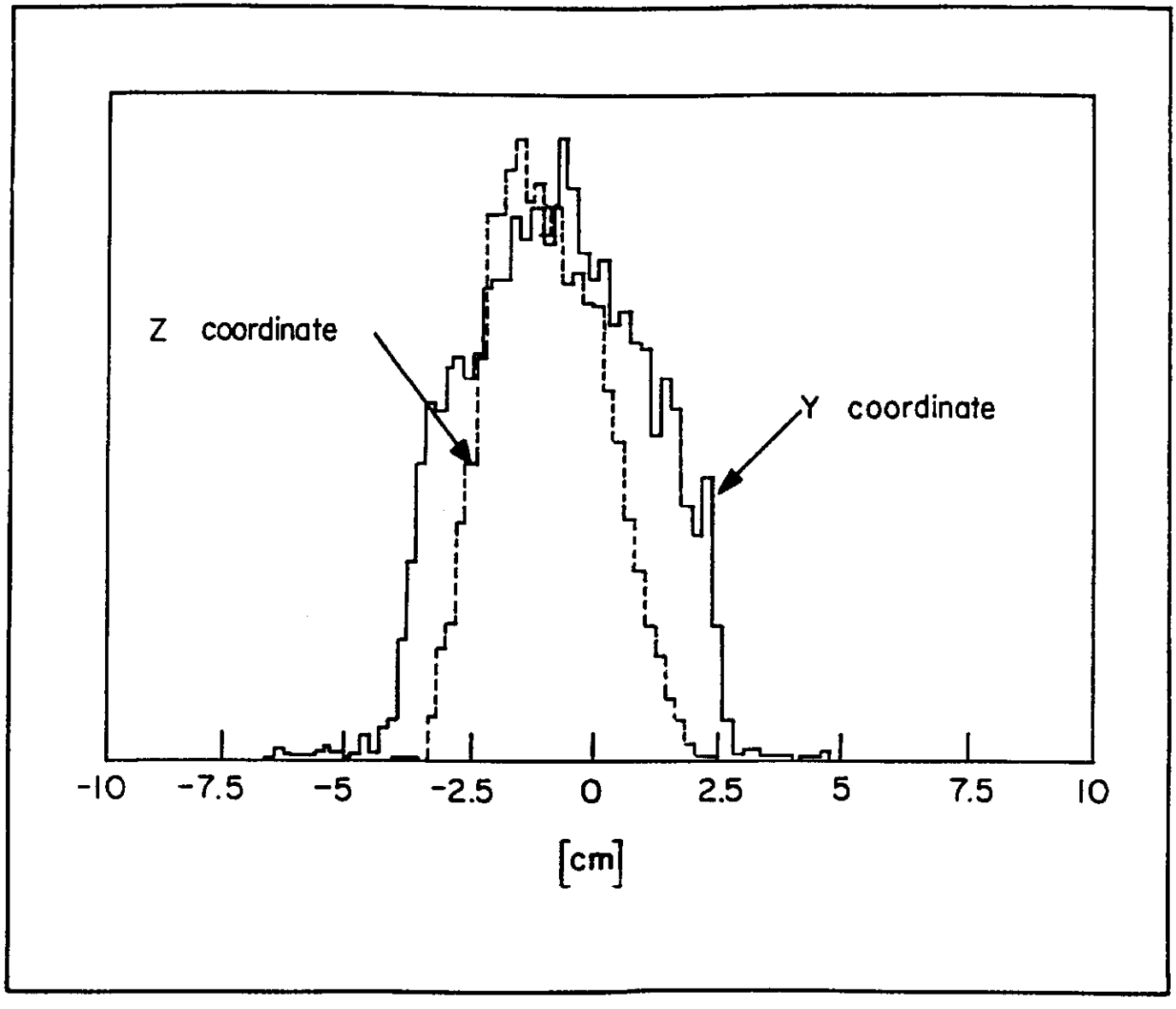

Figure 3

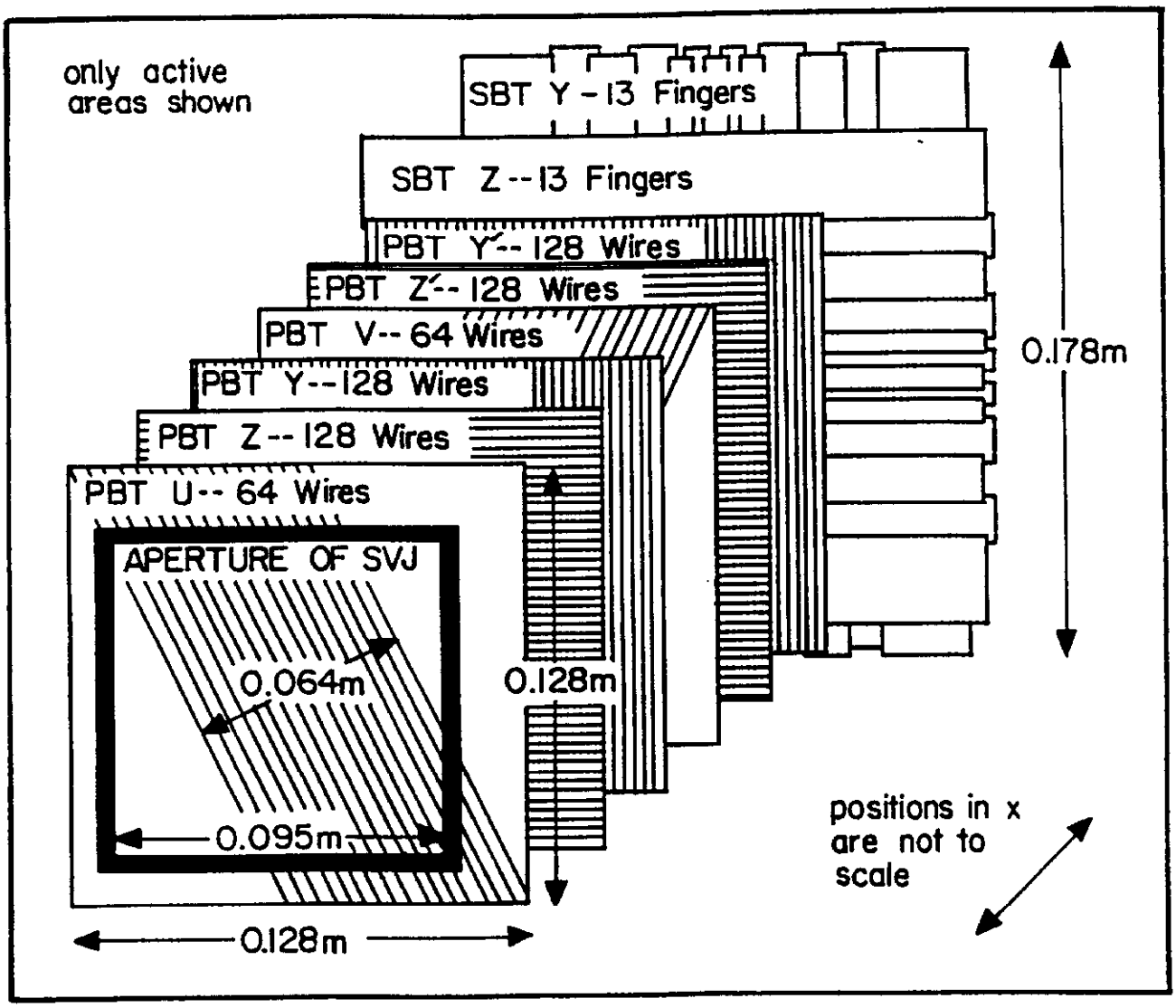
only active
areas shown
SBT Y - 13 Fingers
SBT Z -- 13 Fingers
PBT Y -- 128 Wires
PBT Z -- 128 Wires
PBT V -- 64 Wires
PBT Y -- 128 Wires
PBT Z -- 128 Wires
PBT U -- 64 Wires
APERTURE OF SVJ
0.064m
0.095m
0.128m
0.128m
0.178m
positions in x
are not to
scale

Figure 4

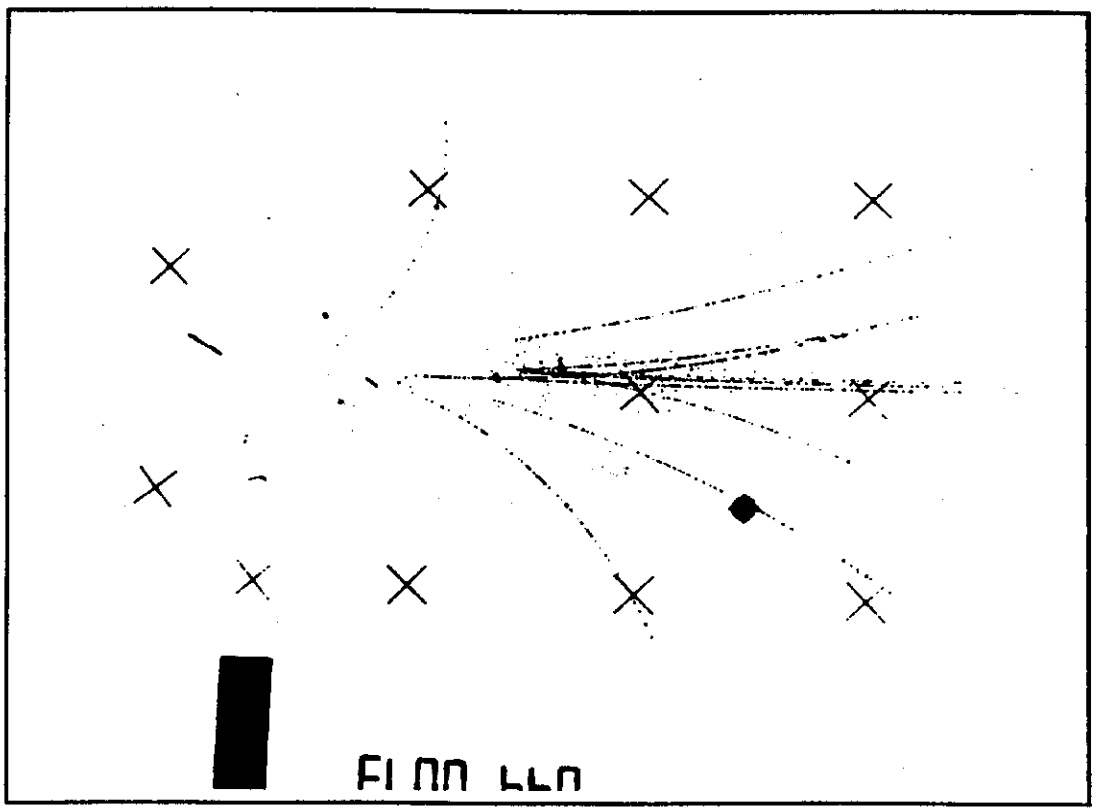

Figure 5

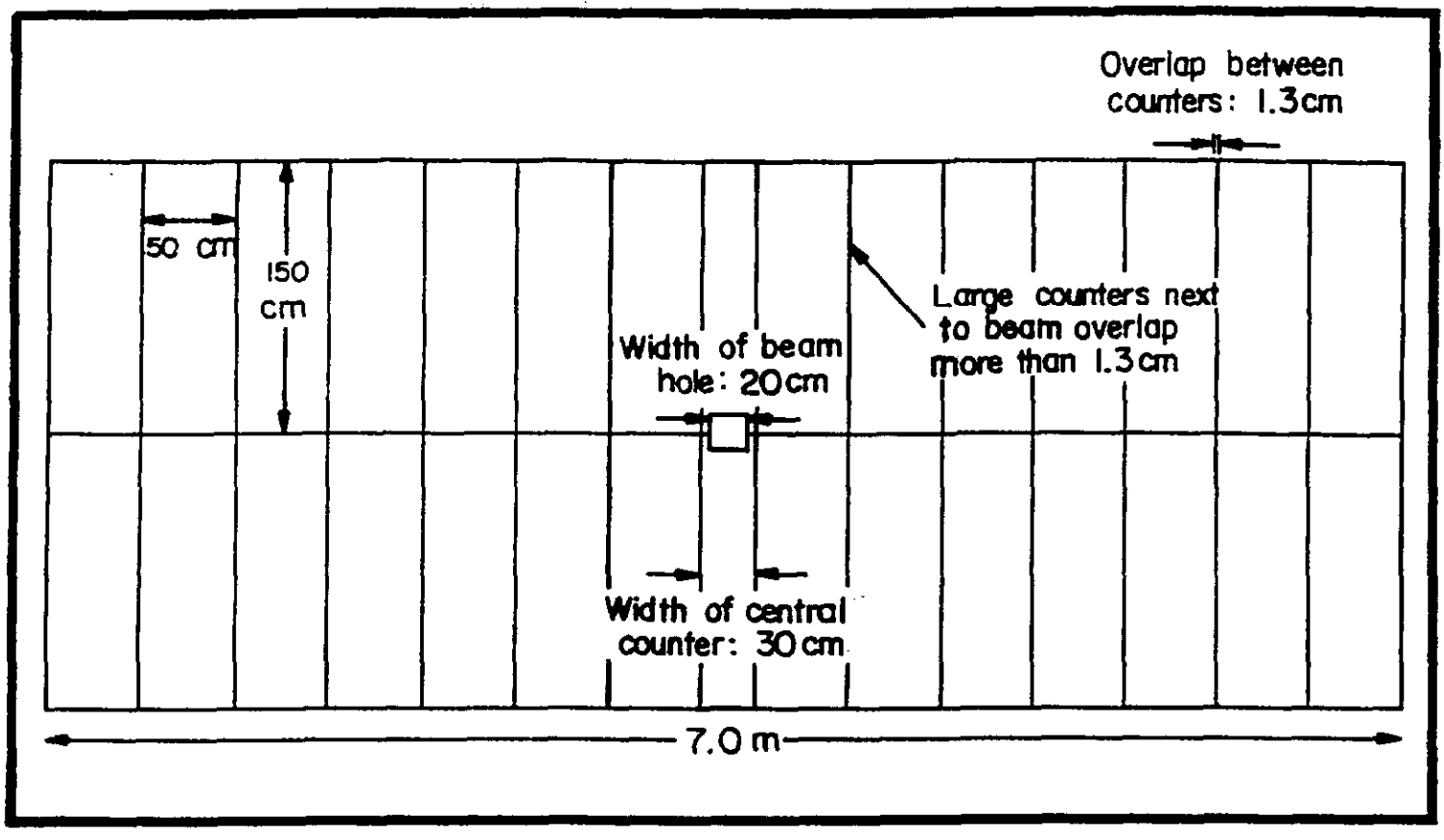
Overlap between
counters: 1.3cm
50 cm
150
cm
Width of beam
hole: 20cm
Large counters next
to beam overlap
more than 1.3cm
Width of central
counter: 30cm
7.0 m

Figure 6

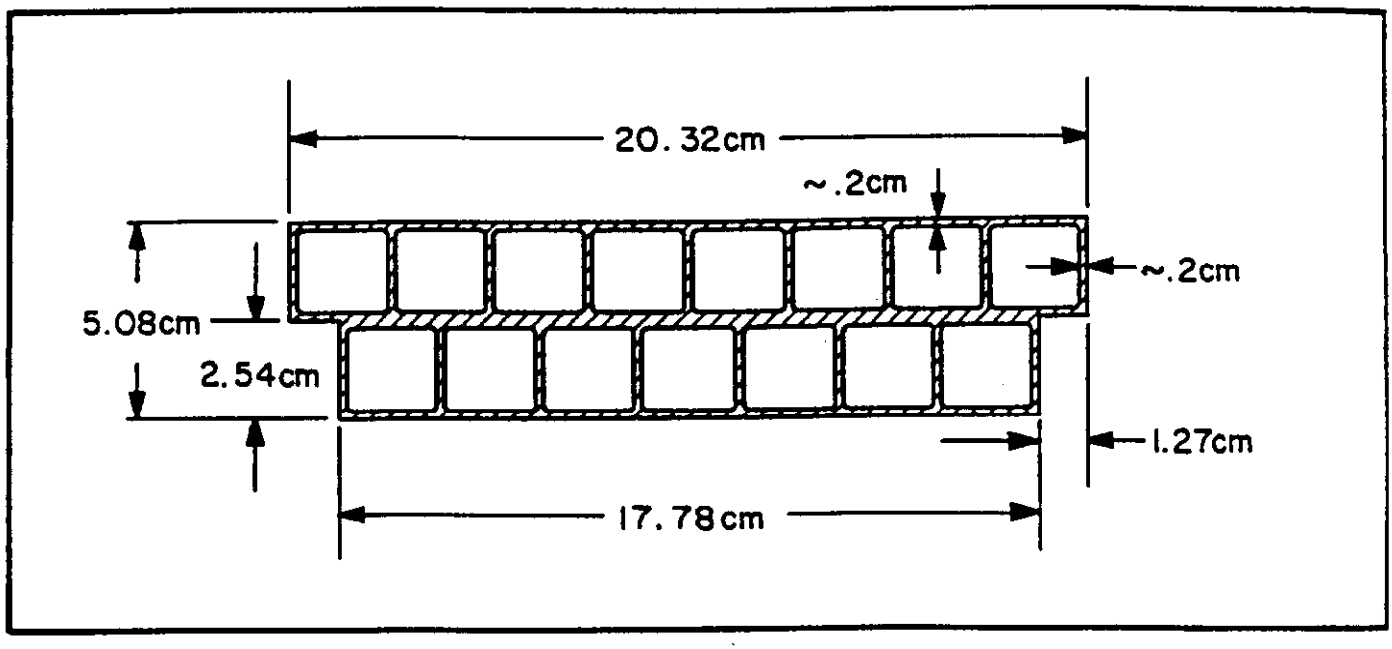

Figure 7

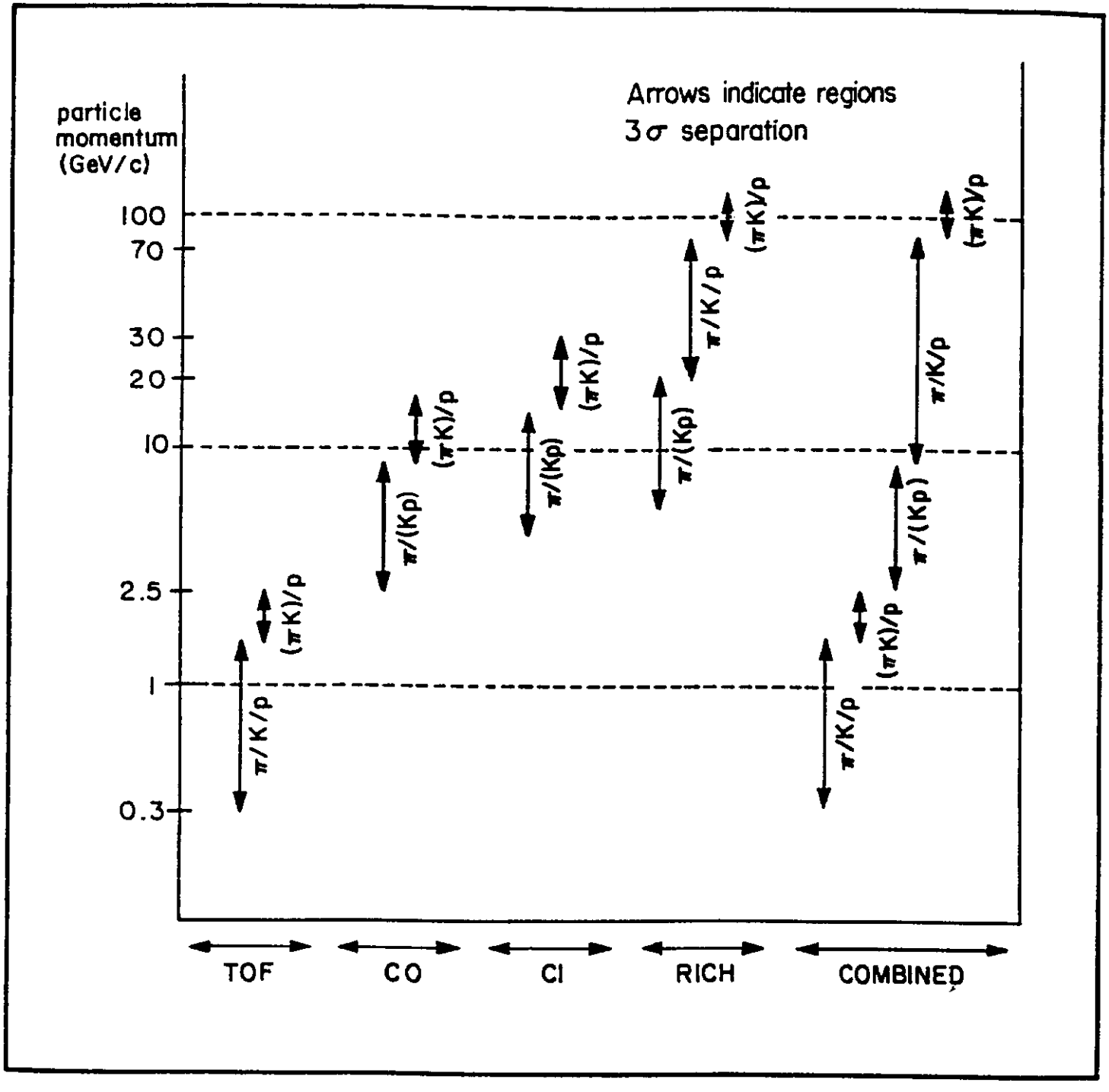
Arrows indicate regions
3σ separation
particle momentum (GeV/c)
100
70
30
20
10
2.5
1
0.3
π/K/ρ
(πK)/ρ
π/(Kρ)
TOF
CO
CI
RICH
COMBINED

Figure 8

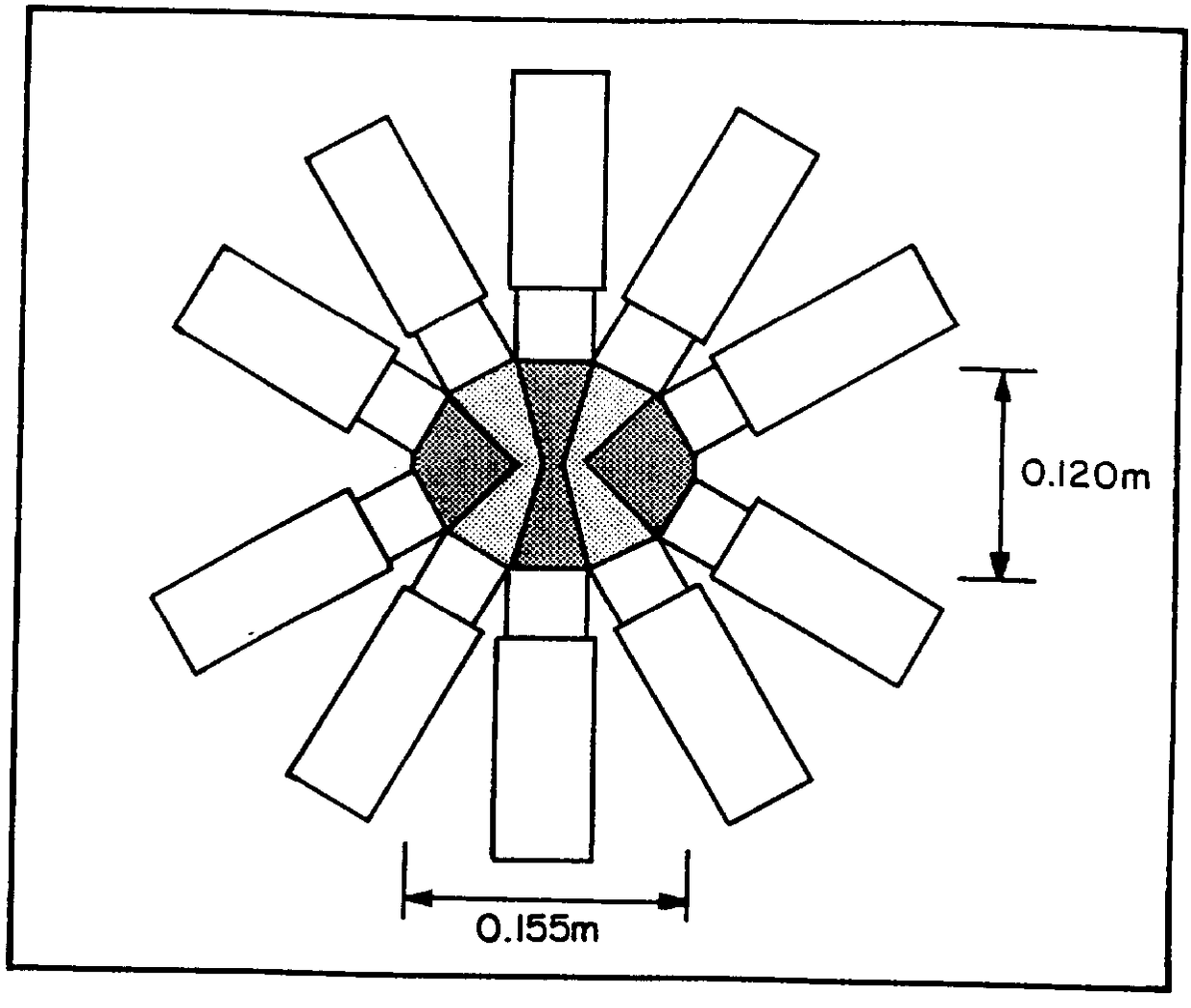

Figure 9

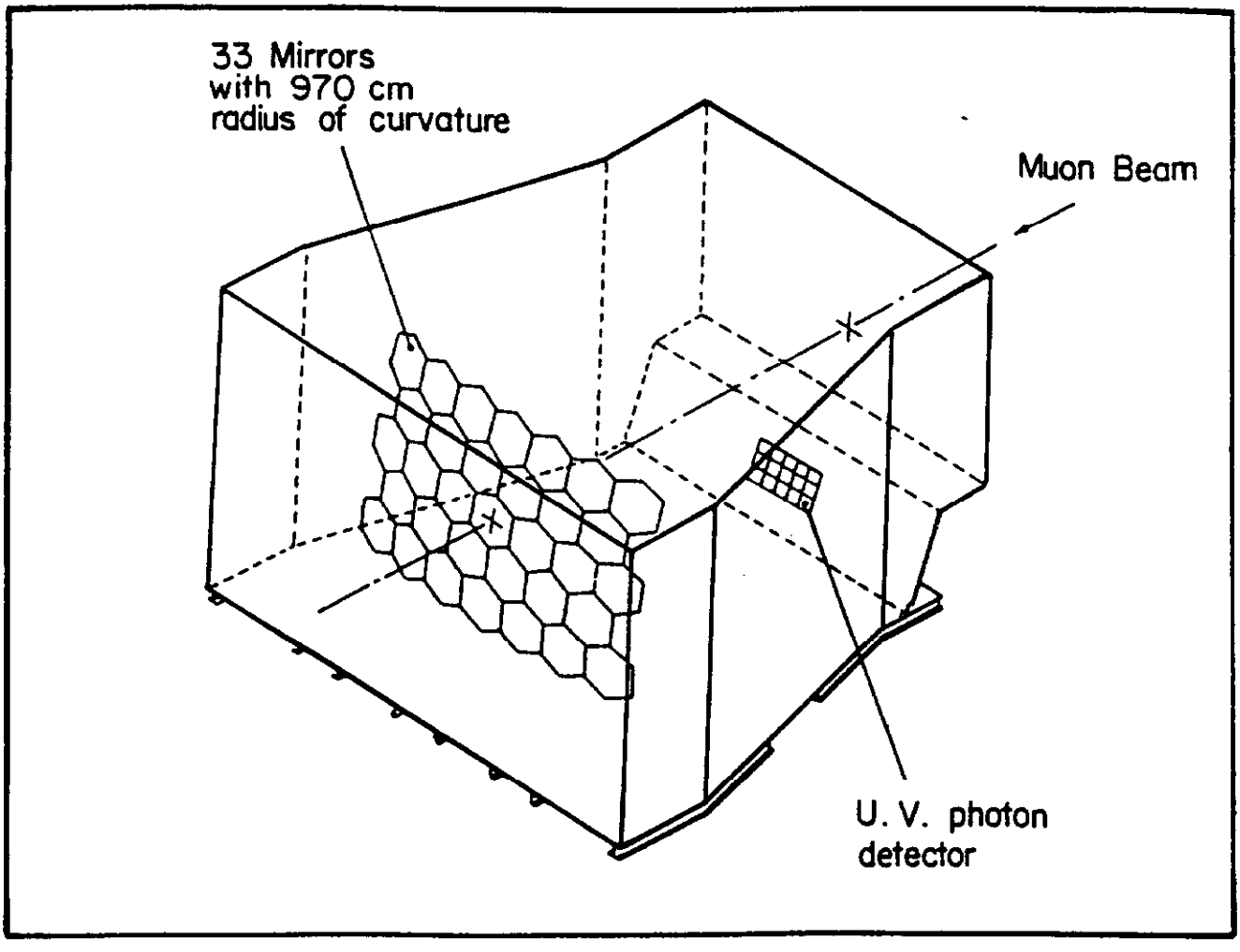
33 Mirrors
with 970 cm
radius of curvature
Muon Beam
U. V. photon
detector

Figure 10

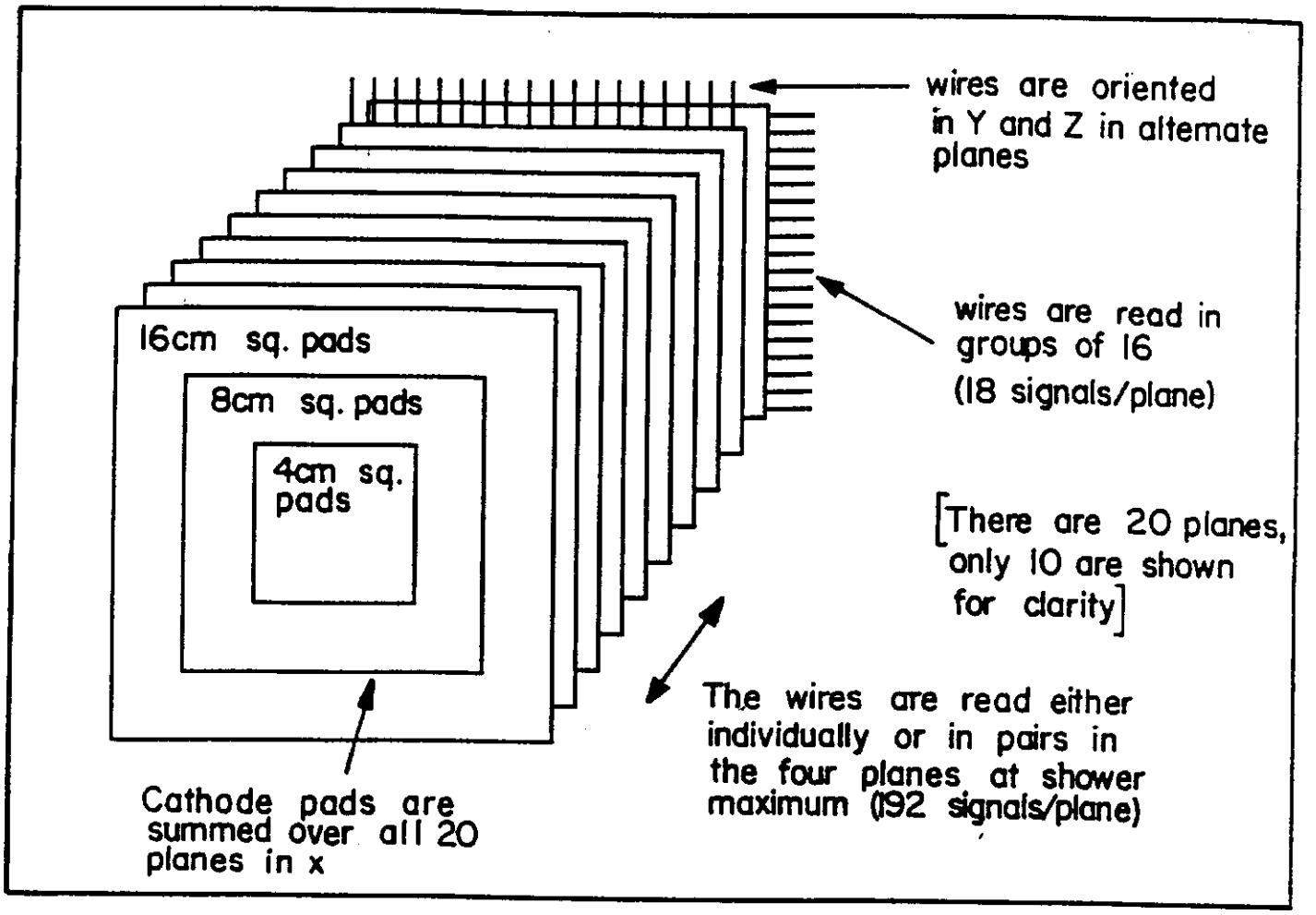
wires are oriented in Y and Z in alternate planes
wires are read in groups of 16 (18 signals/plane)
[There are 20 planes, only 10 are shown for clarity]
16cm sq. pads
8cm sq. pads
4cm sq. pads
The wires are read either individually or in pairs in the four planes at shower maximum (192 signals/plane)
Cathode pads are summed over all 20 planes in x

Figure 11

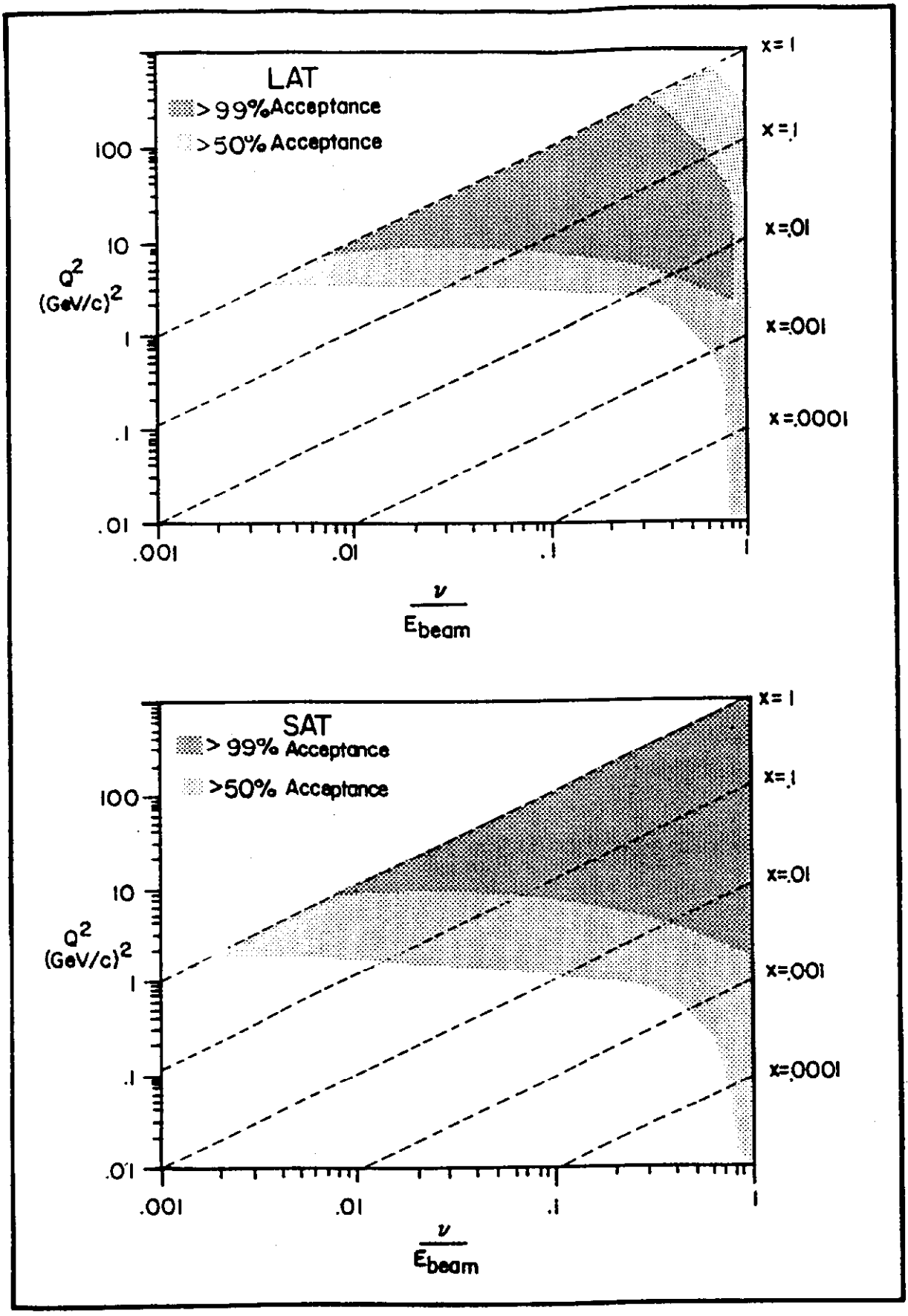
LAT
> 99% Acceptance
> 50% Acceptance
100
10
1
.1
.01
Q^2
$(GeV/c)^2$
.001
.01
.1
1
$\frac{\nu}{E_{beam}}$
x = 1
x = .1
x = .01
x = .001
x = .0001
SAT
> 99% Acceptance
> 50% Acceptance
100
10
1
.1
.01
Q^2
$(GeV/c)^2$
.001
.01
.1
1
$\frac{\nu}{E_{beam}}$
x = 1
x = .1
x = .01
x = .001
x = .0001

Figure 12

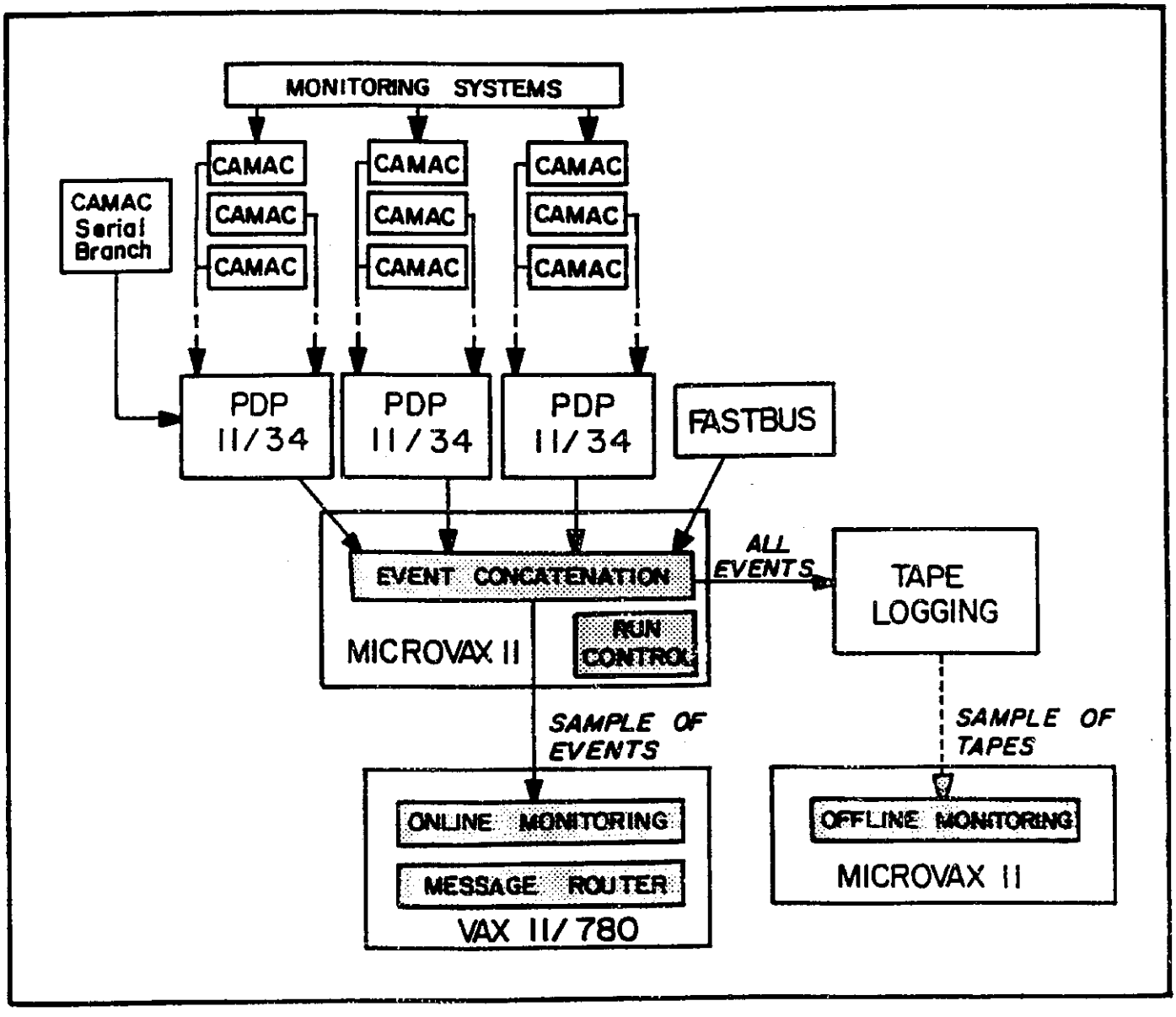
MONITORING SYSTEMS
CAMAC
CAMAC
CAMAC
CAMAC
CAMAC
CAMAC
CAMAC
CAMAC
CAMAC
CAMAC Serial Branch
PDP 11/34
PDP 11/34
PDP 11/34
FASTBUS
EVENT CONCATENATION
MICROVAX II
RUN CONTROL
ALL EVENTS
TAPE LOGGING
SAMPLE OF EVENTS
SAMPLE OF TAPES
ONLINE MONITORING
MESSAGE ROUTER
VAX 11/780
OFFLINE MONITORING
MICROVAX II

Figure 13